



Pseudo-global warming projections of extreme wave storms in complex coastal regions: the case of the Adriatic Sea

Cléa Denamiel¹ · Petra Pranić¹ · Florent Quentin² · Hrvoje Mihanović¹ · Ivica Vilibić¹

Received: 4 February 2020 / Accepted: 24 July 2020 / Published online: 3 August 2020
© Springer-Verlag GmbH Germany, part of Springer Nature 2020

Abstract

This numerical work aims to better understand the behavior of extreme Adriatic Sea wave storms under projected climate change. In this spirit, 36 characteristic events—22 bora and 14 sirocco storms occurring between 1979 and 2019, were selected and ran in evaluation mode in order to estimate the skill of the kilometer-scale Adriatic Sea and Coast (AdriSC) modelling suite used in this study and to provide baseline conditions for the climate change impact. The pseudo-global warming (PGW) methodology—which imposes an additional climatological change to the forcing used in the evaluation simulations, was implemented, for the very first time, for a coupled ocean–wave–atmosphere model and used to assess the behavior of the selected storms under Representative Concentration Pathway (RCP) 4.5 and RCP 8.5 greenhouse gas projections. The findings of this experiment are that, on the one hand, the AdriSC model is found capable of reproducing both the Adriatic waves associated with the 36 storms and the northern Adriatic surges occurring during the sirocco events and, on the other hand, the significant wave heights and peak periods are likely to decrease during all future extreme events but most particularly during bora storms. The northern Adriatic storm surges are in consequence also likely to decrease during sirocco events. As it was previously demonstrated that the Adriatic extreme wind-wave events are likely to be less intense in a future warmer climate, this study also proved the validity of applying the PGW methodology to coupled ocean–wave–atmosphere models at the coastal and nearshore scales.

Keywords Adriatic Sea · Extreme storms · Pseudo-global warming · Extreme waves · Storm surges

1 Introduction

In the past decade, atmospheric regional climate projections—with typical resolutions of 12 to 50-km, have been used in the Mediterranean Sea and most particularly in the Adriatic Sea (Fig. 1a) in a wide range of impact studies, such as the assessment of future wind (e.g. Bellafiore et al. 2012; Belušić Vozila et al. 2019), wave (e.g. Lionello et al. 2012a; Benetazzo et al. 2012; Bonaldo et al. 2017) and storm surge (e.g. Lionello et al. 2012b; Androulidakis et al. 2015; Mel et al. 2013) climates or the characterization of climate-related hazards (i.e. flooding, extreme wave conditions, coastal vulnerability and erosion processes) in the northern

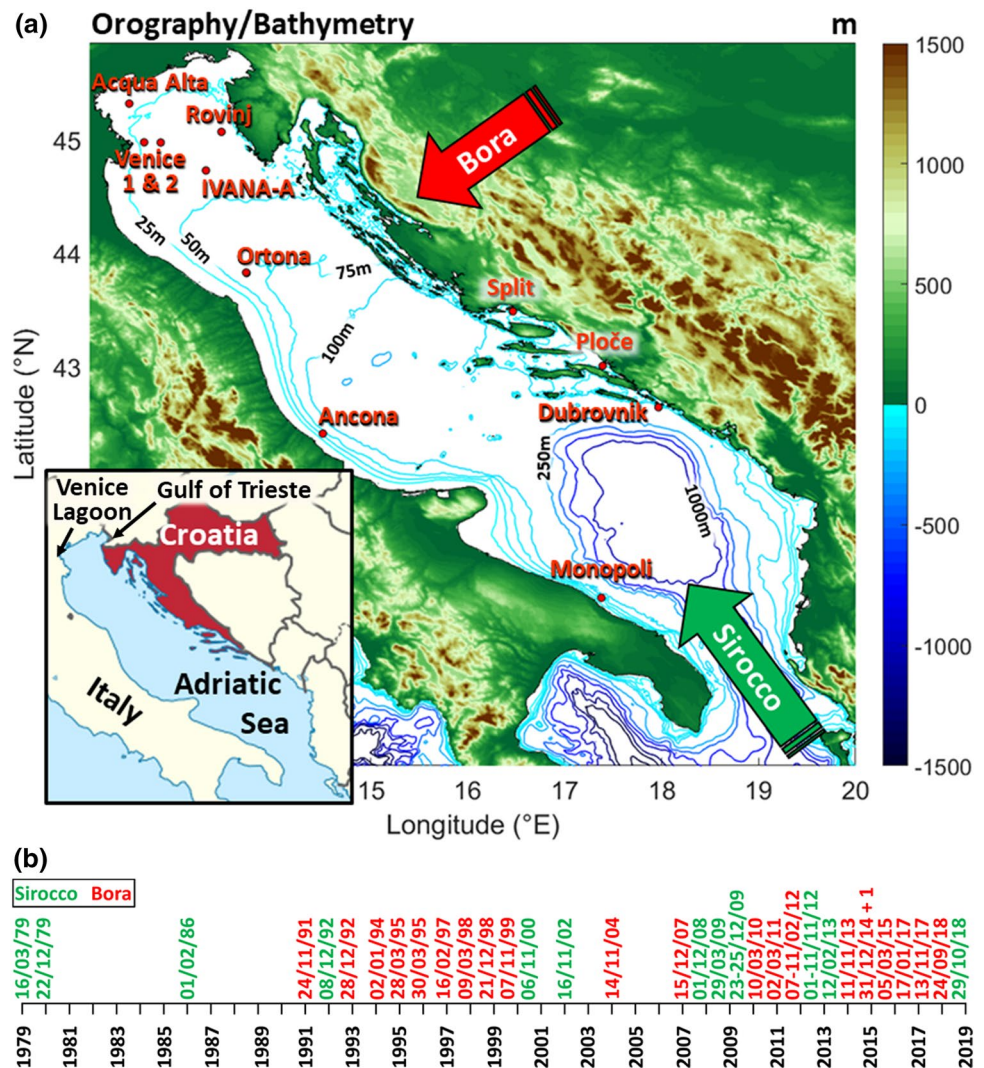
Adriatic (e.g. Rizzi et al. 2017; Torresan et al. 2019). In particular, Benetazzo et al. (2012) demonstrated that, in the Adriatic Sea, the observed seasonal wave characteristics could be numerically reproduced at the regional scale and the intensity of the strongest winds (i.e. the so-called bora and sirocco events; Brzović and Strelec Mahović 1999; Grisogono and Belušić 2009), and in consequence of the waves, was likely to decrease by the end of the twenty-first century. The study also highlighted that additional research should focus on distinguishing the effect of climate change on extreme bora and sirocco events, which lead to respectively strong air–sea interactions (e.g. Pullen et al. 2006; Janeković et al. 2014; Ličer et al. 2016) impacting the Adriatic thermohaline circulation (Vilibić et al. 2013) and high waves potentially associated with storm surges in the northern Adriatic (Vilibić et al. 2017; Bajo et al. 2019)—more particularly flooding in the Venice Lagoon (Trigo and Davies 2002; Cavaleri et al. 2010), or capable of moving large boulders (weighting up to a ton) along the Croatian coastline (Biolchi et al. 2019a, b).

✉ Cléa Denamiel
cdenamie@izor.hr

¹ Institute of Oceanography and Fisheries, Šetalište I.
Meštrovića 63, 21000 Split, Croatia

² SeaTech, Ecole d'ingénieurs, Université de Toulon,
CS 60584 83041 Toulon Cedex 9, France

Fig. 1 **a** Location of the different Adriatic Sea wave measurements along the Italian and Croatian coastline and **b** selected 36 one-day extreme wave events during the 1979–2019 period—depending on the wind conditions (bora or sirocco) schematized by arrows in the map, used for the SWAN model evaluation. The notation + 1 (**b**) means that the 01/01/2015 event is also selected



However, due to the complex orography of the elongated semi-enclosed Adriatic basin surrounded by mountains and associated with bathymetries evolving from a really shallow and wide shelf (300 km in length with less than 80 m in depth) in the north to a deep pit (about 1200 m depth) in the south (Fig. 1a), the evolution of the extreme bora and sirocco wind patterns, and their impact on extreme waves and storm surges, can only be achieved via high-resolution limited-area atmospheric models (e.g. Pasarić et al. 2007; Klaić et al. 2009; Prtenjak and Belušić 2009; Prtenjak et al. 2010; Ricchi et al. 2016; Cavaleri et al. 2018) forcing sea-state and surge models (e.g. Cavaleri et al. 2010, 2019). Additionally, in the recent years, the use of very high-resolution (i.e. kilometer-scale, also known as convection-permitting) regional climate models in atmospheric studies—in particular via the so-called pseudo-global warming (PGW) downscaling method (Schär et al. 1996; Rasmussen et al. 2011), has been proven to greatly improve the future projection of precipitations and convective storms (Pan et al. 2011; Kendon et al.

2014; Tolle et al. 2014; Argueso et al. 2014; Rasmussen et al. 2014; Ban et al. 2014; Prein et al. 2015; Fosser et al. 2016; Kendon et al. 2017). Though, because of their tremendous computational costs, such high-resolution applications have not yet been developed for coupled ocean–atmosphere models.

The present paper thus aims at both (1) implementing and testing the PGW methodology—already used in kilometer-scale atmospheric climate studies, for a complex kilometer-scale atmosphere–wave–ocean modelling suite and (2) quantifying the changes of the Adriatic wave extremes, and their associated storm surges during sirocco events, between present-day (for the 1979–2019 period) conditions and future climate projections (for the 2060–2100 period) for two greenhouse gas scenarios: Representative Concentration Pathway 4.5 (RCP 4.5) and Representative Concentration Pathway 8.5 (RCP 8.5). To this purpose, Sect. 2 first describes in detail the newly developed Adriatic Sea and Coast (AdriSC) modelling suite (Denamiel et al. 2019) used

in this study, the set of sirocco and bora storms as well as the wave and sea-level measurements selected in the Adriatic Sea for the 1979–2019 period and, finally, the implementation of the PGW methodology for the ocean–wave–atmosphere AdriSC model. Then, the evaluation of the AdriSC model and the statistical analysis of the climate change impact on the Adriatic extreme waves and storm surges under RCP 4.5 and RCP 8.5 scenarios are presented in Sect. 3. Finally, the validity and limitations of the methodology and results derived in this numerical experiment are discussed in Sect. 4 and some conclusions about the feasibility of using such an approach for long-term climate studies are presented.

2 Model, data and methods

2.1 The AdriSC modelling suite

The Adriatic Sea and Coast (AdriSC) modelling suite (Denamiel et al. 2019) has been recently developed with the aim to accurately represent the processes driving the atmospheric and oceanic circulation at different temporal and spatial scales over the Adriatic and northern Ionian Sea. In this spirit, the AdriSC modelling suite is based on two different modules: a basic module which provides atmospheric and oceanic baroclinic circulation at the deep sea and coastal scales, and a dedicated nearshore module which is used to better reproduce atmospherically-driven extreme events.

The basic module of the AdriSC suite rely on the use and development of the Coupled Ocean–Atmosphere–Wave–Sediment Transport (COAWST) modelling system (Warner et al. 2010). It is built around the Model Coupling Toolkit (MCT) which exchanges data fields and dynamically couples the Weather Research and Forecasting (WRF) atmospheric model, the Regional Ocean Modeling System (ROMS) and the Simulating WAVes Nearshore (SWAN) model. The basic module (Table 1) is set-up with two different nested grids of 15-km and 3-km resolution used in the WRF model and covering respectively the central

Mediterranean area and the Adriatic-Ionian region, as well as two different nested grids of 3-km and 1-km resolution used for both ROMS and SWAN models and covering respectively the Adriatic-Ionian region (similarly to the WRF 3-km grid) and the Adriatic Sea only.

In the nearshore module, the fully coupled ADCIRC-SWAN unstructured model (Dietrich et al. 2012)—covering the entire Adriatic Sea with resolutions ranging from 5-km in the deepest part of the domain to 10 m at the coast (Table 1), is forced every minute with the off-line atmospheric results of a dedicated high-resolution WRF 1.5-km grid. In more details, the hourly results from the WRF 3-km grid obtained with the basic module are first downscaled to a WRF 1.5-km grid covering the Adriatic Sea and the hourly sea surface elevation from the ROMS 1-km grid, the 10-min spectral wave results from the SWAN 1-km grid and finally the 1-min results from the WRF 1.5-km grid are then used to force the unstructured mesh of the ADCIRC-SWAN model.

The AdriSC modelling suite is installed and fully tested on the European Centre for Middle-range Weather Forecast (ECMWF) high-performance computing facilities. Table 1 provides a summary of the AdriSC set-up while more details can be found in Denamiel et al. (2019).

In this study, in order to reproduce the strongest historical wave storms which took place in the Adriatic Sea during the 1979–2019 period and to assess their behavior under climate change projections (RCP 4.5 and RCP 8.5 scenarios), the SWAN model—originally unused in the AdriSC modelling suite, was set-up in both modules to be coupled with the ocean and atmosphere models (i.e. WRF, ROMS, ADCIRC). In the actual configuration, the third generation SWAN model is used with backward space and time propagation schemes, default initial condition, dissipation from whitecapping by Komen et al. (1984) and Madsen bottom friction (Madsen et al. 1988). The wave model receives forcing from WRF 3-km (wind fields) and ROMS 3-km/1-km (ocean surface currents, sea-level and friction) every 10 min in the basic module and from WRF 1.5-km (wind fields) and ADCIRC (ocean barotropic currents, sea-level and friction) every minute in the nearshore module. In addition,

Table 1 Summary of the AdriSC modelling suite main features

Models	Basic module				Nearshore module	
	Atmosphere		Ocean		Atmosphere	Ocean
	WRF		ROMS-SWAN		WRF	ADCIRC-SWAN
Number of domains	2		2		1	1
Resolution	15 km	3 km	3 km	1 km	1.5 km	5 km to 10 m
Initial and boundary conditions	ERA-Interim		MEDSEA ERA-Interim		WRF 3-km	ROMS-SWAN 1-km
Duration of run (with d0 the day of the event at 0 h)	72 h from d0 – 48 h to d0 + 24 h				36 h from d0 – 12 h to d0 + 24 h	
Frequency of outputs	Hourly				1-min	

the computation of the bottom stress of the ocean models (respectively ROMS and ADCIRC) was updated in order to account for the spatial distribution of the sediment grain size at the bottom of the Adriatic Sea extracted from the Adriatic Seabed database (Jenkins et al. 2005) and the wave effects. For the evaluation runs, during the 1979–2019 period, in order to reproduce the historical storms as accurately as possible, the basic module was set-up to run for 3 days. Initial conditions and boundary forcing were provided the 6-hourly ERA-Interim re-analysis fields (Dee et al. 2011; Balsamo et al. 2015), either the monthly or the daily re-analysis MEDSEA-Ocean fields (Pinaridi et al. 2003), depending on whether the storm took place before or after the 1st of January 1987, and either the 6-hourly ERA-Interim wave fields or the hourly MEDSEA-Wave fields (Ravdas et al. 2018), depending on whether the storms took place before or after the 1st January 2006. The nearshore module, forced by the results of the basic module, was set-up to run for the last day and half of the basic module simulations.

As an in-depth sensitivity study of the impact of model resolution on the wave and storm surge representation is out of scope in this work, the advantages of using kilometer scale model in the atmosphere and unstructured meshes in the ocean is briefly discussed in Appendix 1. However, hereafter, only the last 24-h 1-min wave and sea-level results of the nearshore module extracted from respectively the unstructured SWAN model (referred as AdriSC unSWAN in this study) and the ADCIRC model are analyzed.

2.2 Documented historical extreme wave storms in the Adriatic Sea

In the Adriatic Sea, only two most frequent winds—bora and sirocco (Fig. 1a), can produce fetches large enough to drive extreme wave storms (Pomaro et al. 2017). The bora is a cold east-northeast wind which flows through eastern Adriatic mountain passes, being particularly severe along the Croatian coastline where its intensity sometimes surpasses 30 m s^{-1} and its gust reaches up to 70 m s^{-1} (e.g. Jiang and Doyle 2005; Kuzmić et al. 2005; Belušić and Klaić 2006; Gohm et al. 2008; Grisogono and Belušić 2009; Trošić 2015). Continuous gale force ($> 15 \text{ m s}^{-1}$) bora winds are most common during the cold season (November through March) and have an average duration of 12 h with rare events that can last up to 2 days. The sirocco is a warm southeast wind originating from North Africa, blowing over the Mediterranean Sea and sometimes affecting the Adriatic Sea, being channelized by the surrounding mountains, with gust reaching more than 30 m s^{-1} (e.g. Poje 1992; Jurčec et al. 1996; Penzar et al. 2001; Pasarić and Orlić 2004). Although sirocco winds are not as strong as the bora, continuous gale force events occur more frequently between October and March,

usually lasting 10–12 h—with rare occurrences as long as 36 h, and often bring rain—sometimes mixed with Saharan dust (Cushman-Roisin et al. 2001). Both sirocco and bora episodes may vary in intensity and spatial coverage, extending either over the whole Adriatic or just a part or being conjoined, with sirocco blowing in the southern and bora in the northern Adriatic. Finally, in terms of extreme conditions, as sirocco winds can produce extended fetch, contrarily to the bora winds which are fetch-limited, the largest wave heights were recorded in the northern Adriatic during extreme sirocco events (Leder et al. 1998; Bertotti et al. 2011; Pomaro et al. 2017). These waves can be associated with extreme storm surges in the Venice Lagoon, the Gulf of Trieste (Fig. 1a) and the whole northern Adriatic (Lionello et al. 2012a; Međugorac et al. 2015).

In this study, in order to perform the evaluation of the AdriSC nearshore module, the choice of the studied extreme events was mostly driven by the available information and measurements recorded during the 1979–2019 period. For the sirocco events, the 14 selected storms (Fig. 1b) were extracted from the long-term record of the Venice extreme flooding (<https://www.comune.venezia.it/it/content/le-acque-alte-eccezionali>). For the bora events, only 22 of the most recent extreme storms were selected (Fig. 1b) as more wave measurements became available in the Adriatic Sea at the end of the twentieth century (more details on the selected bora events are provided in Appendix 2). The majority of the selected bora events peaked in the northern Adriatic, where bora wind is the strongest (Grisogono and Belušić 2009). The set of wave measurements (Table 2)—used to evaluate the skills of the AdriSC nearshore module to reproduce the 36 selected storms, spans between 1979 and 2019 and consists in 6 stations along the Italian coast—Acqua Alta tower from Pomaro et al. (2018), Venice 1 (only for the significant wave height measurements) from the Copernicus Marine Environment Monitoring Service (ftp://my.cmems-du.eu/Core/INSITU_GLO_WAVE_REP_OBSERVATIONS_013_045/history/mooring/) and Venice 2, Ortona, Ancona, Monopoli from the Italian Data Buoy Network managed by ISPRA (Bencivenga et al. 2012), 4 stations along the Croatian coastline—Rovinj, Split, Ploče and Dubrovnik, from the Croatian Hydrographic Institute (Hrvatski hidrografski institut—HHI), and one station in the middle of the northern Adriatic shelf—IVANA-A also from HHI. However, it should be noticed that storm coverage is about 5 times higher from the Italian than the Croatian measurements (Table 2). In addition, concerning the extreme storm surges associated with the sirocco events, two long-term hourly sea-level measurements extracted between 1979 and 2019 from tide gauges located respectively in the Venice Lagoon (at Punta Della Salute, 45.4310° N and 12.3364° E , maintained by ISMAR Venezia) and in the Gulf of Trieste (at 45.6544° N and 13.7561° E , maintained by ISMAR

Table 2 Adriatic Sea wave buoy data available along the Italian and Croatian coastlines between 1979 and 2019

Name	Location	Period of measurements	Sampling	Events ^a
Acqua Alta	12.5088° E 45.3138° N	01.01.1979– 01.01.2018	3 h	33
Venice 1	12.6627° E 44.9735° N	01.06.2013– 01.01.2015	1 h	3
Venice 2	12.8330° E 44.9717° N	01.06.2002– 01.01.2015	1 h	9
Ortona	14.5056° E 42.4150° N	01.07.1989– 19.05.2011	1 h	17
Ancona	13.7144° E 43.8297° N	10.03.1999– 07.11.2014	1 h	13
Monopoli	17.3767° E 40.9750° N	01.07.1989– 01.01.2015	1 h	19
IVANA-A	13.2997° E 44.7262° N	01.11.2007– 13.05.2010	30 min	6
Rovinj	13.4599° E 45.0655° N	11.05.2018– 01.01.2019	30 min	1
Split	16.4650° E 43.4883° N	29.10.2007– 01.01.2019	30 min	5
Ploče	17.3913° E 43.0096° N	09.12.2016– 01.01.2019	30 min	4
Dubrovnik	17.9667° E 42.6460° N	06.04.2017– 01.01.2019	30 min	3

^aNumber of the selected 36 storms covered by the measurements

Trieste) were also used to evaluate the skill of the AdriSC nearshore module.

2.3 Pseudo-global warming methodology

The two major challenges posed by performing kilometer-scale climate projection simulations are, on the one hand, the relative slowness of the AdriSC modelling suite (a month of results produced per day with the basic module alone), and on the other hand, the low temporal and spatial resolutions (only few vertical levels for daily or monthly data) of the coupled regional climate model (RCM) results available to provide boundary conditions to the WRF 15-km and ROMS 3-km models. To address these concerns, the projection of the extreme Adriatic Sea wave events for the RCP 4.5 and RCP 8.5 scenarios is performed, in this study, via a pseudo-global warming (PGW) method. The principle of the PGW simulations—as first introduced by Schär et al. (1996) and described in details by Rasmussen et al. (2011), Kröner et al. (2017) and Brogli et al. (2019a, b), is to impose an additional climatological change (e.g. a temperature change ΔT representative of the increase in temperature between past and future climate) to the forcing used to produce the evaluation runs.

In the Mediterranean Sea, one of the specific aim of the Med-CORDEX experiment ([https://www.medcordex.](https://www.medcordex.eu/)

<https://www.medcordex.eu/>)—part of the Coordinated Regional Climate Downscaling Experiment (CORDEX) initiative (<https://esg-dn1.nsc.liu.se/search/cordex/>) which coordinates the production of climate change projections at the regional scale (Giorgi et al. 2009; Giorgi and Gutowski 2015), is to provide coupled ocean–atmosphere regional model results. The RCMs of the Med-CORDEX ensemble are based on several numerical models running in coupled or uncoupled mode and forced by different Global Climate Models (GCMs). However, at the time of this study, due to a reported issue with the CNRM-CM5 CMIP5 GCM forcing for the historical run (that removes reliability of this product, https://www.medcordex.eu/warnings/Communication-Issue-Files_CNRM-CM5_historical_6hLev_en.pdf), the only coupled results publicly available—with high enough temporal and spatial resolutions for the historical period (1950–2005) and the two climate scenarios RCP 4.5 and RCP 8.5 (2006–2100), were those of the LMDZ4-NEMOMED8 RCM model (Hourdin et al. 2006; Beuquier et al. 2010) forced by the IPSL-CM5A-MR GCM model (simulations r1i1p1). These results—defined as two continuous LMDZ4-NEMOMED8 simulations (1950–2100) extending the historical run with either the RCP 4.5 or the RCP 8.5 runs, are referred as SCEN 4.5 and SCEN 8.5, respectively, and used hereafter to force the PGW simulations. The PGW climatological changes derived from SCEN 4.5 and SCEN 8.5 between the 1979–2019 and the 2060–2100 periods are thus tested in this study.

Finally, the key development of this work is the extension of the PGW method—which had till now only been used in atmospheric models, to the ocean models and more particularly to the AdriSC modelling suite. For the atmosphere, as described in many previous studies (Pan et al. 2011; Kendon et al. 2014; Tolle et al. 2014; Argueso et al. 2014; Rasmussen et al. 2014; Ban et al. 2015; Prein et al. 2015; Fosser et al. 2016; Kendon et al. 2017), the ERA-Interim air temperature (T^{ERAI}), relative humidity (RH^{ERAI}) and horizontal wind velocities $\mathbf{V}^{ERAI} = (V_x^{ERAI}, V_y^{ERAI})$ defined on 37 atmospheric pressure levels (p) are modified between 1000 and 70 hPa with respectively $\Delta T(t_{clim}, x, y, p)$, $\Delta RH(t_{clim}, x, y, p)$ and $\Delta \mathbf{V} = (\Delta V_x(t_{clim}, x, y, p), \Delta V_y(t_{clim}, x, y, p))$ derived from SCEN 4.5 and SCEN 8.5 by subtracting the atmospheric results from the 1979–2019 period to those of the 2060–2100 period and producing 6-hourly three-dimensional climatologic changes for the 366 days of the year (t_{clim}). The WRF 15-km boundary and initial conditions of the PGW simulations (T^{SCEN} , RH^{SCEN} , V_x^{SCEN} and V_y^{SCEN}) are thus given by:

$$\begin{aligned}
 T^{SCEN}(t, x, y, p) &= T^{ERAI}(t, x, y, p) + \Delta T(t_{clim}, x, y, p) \\
 RH^{SCEN}(t, x, y, p) &= RH^{ERAI}(t, x, y, p) + \Delta RH(t_{clim}, x, y, p) \\
 V_x^{SCEN}(t, x, y, p) &= V_x^{ERAI}(t, x, y, p) + \Delta V_x(t_{clim}, x, y, p) \\
 V_y^{SCEN}(t, x, y, p) &= V_y^{ERAI}(t, x, y, p) + \Delta V_y(t_{clim}, x, y, p)
 \end{aligned} \tag{1}$$

In order to adjust the height of the surfaces of constant pressure to the temperature and relative humidity changes, the geopotential—depending on the virtual temperature T_v^{SCEN} , the ERA-Interim geopotential ϕ^{ERA-I} at the reference pressure $p_{ref} = 1000$ hPa and the gas constant R , is recalculated as follow:

$$\phi^{SCEN}(t, x, y, p) = \phi^{ERA-I}(t, x, y, p_{ref}) - \int_{p_{ref}}^p \frac{RT_v^{SCEN}}{p} dp \quad (2)$$

Finally, the 2-m air temperature change ΔT_S derived from SCEN 4.5 and SCEN 8.5 runs is used to adjust the ERA-Interim surface (ground and 2-m air) temperatures (T_S^{ERA-I}) such as:

$$T_S^{SCEN}(t, x, y) = T_S^{ERA-I}(t, x, y) + \Delta T_S(t_{clim}, x, y) \quad (3)$$

The developed methodology for the ocean follows the principles of the PGW for the atmosphere. In this study, the MEDSEA ocean temperature (T^{MEDSEA}), salinity (S^{MEDSEA}) and currents (V_x^{MEDSEA} , V_y^{MEDSEA}) defined on 72 unevenly spaced vertical levels (z), are thus modified with respectively $\Delta T(t_{clim}, x, y, z)$, $\Delta S(t_{clim}, x, y, z)$ and $\Delta V = (\Delta V_x(t_{clim}, x, y, z), \Delta V_y(t_{clim}, x, y, z))$ derived from SCEN 4.5 and SCEN 8.5 ocean results to produce daily climatologic changes (t_{clim}) for the 366 days of the year. The ROMS 3-km boundary and initial conditions of the PGW simulations (T^{SCEN} and S^{SCEN}) are thus given by:

$$\begin{aligned} T^{SCEN}(t, x, y, z) &= T^{MEDSEA}(t, x, y, z) + \Delta T(t_{clim}, x, y, z) \\ S^{SCEN}(t, x, y, z) &= S^{MEDSEA}(t, x, y, z) + \Delta S(t_{clim}, x, y, z) \\ V_x^{SCEN}(t, x, y, z) &= V_x^{MEDSEA}(t, x, y, z) + \Delta V_x(t_{clim}, x, y, z) \\ V_y^{SCEN}(t, x, y, z) &= V_y^{MEDSEA}(t, x, y, z) + \Delta V_y(t_{clim}, x, y, z) \end{aligned} \quad (4)$$

In the ocean, the static stability depends on the density (ρ) and the vertical variations of the local potential density (σ_n) such as:

$$E(x, y, z) = -\frac{1}{\rho(x, y, z)} \frac{\delta \sigma_n}{\delta z} \quad (5)$$

The stability of the ocean forcing (at the boundaries and for the initial condition) is thus ensured by imposing $E^{SCEN} \geq 0$ at all vertical levels. Finally, the sea surface elevation change Δssh derived from SCEN 4.5 and SCEN 8.5 runs is used to adjust the MEDSEA surface layer (ssh^{MEDSEA}) such as:

$$ssh^{SCEN}(t, x, y) = ssh^{MEDSEA}(t, x, y) + \Delta ssh(t_{clim}, x, y) \quad (6)$$

The temperature changes (ΔT) imposed at the boundaries of both the ocean and atmosphere models are illustrated in Fig. 2. The vertical variations of the spatially- and

time- averaged ΔT presented in Fig. 2b clearly show that, near the surface of the earth, the differences in temperature between scenarios RCP 4.5 and RCP 8.5 reach more than 1.5 °C (for both the ocean and the atmosphere). For the ocean, no significant difference between the two scenarios is seen below depth of 1000 m. For the atmosphere, this difference only starts to decrease above 400 hPa and is minimized above 100 hPa. In addition, the time variations of the spatially-averaged ΔT for scenario RCP 8.5 (Fig. 2c) highlights that the temperature change imposed to the atmosphere at 2 m height is, most of a year, at least 0.5 °C higher than the one imposed to the sea surface temperature. Finally, Fig. 2d, e present the vertical variations of the temporally-averaged ΔT along the southern and western boundaries of both the atmosphere and ocean models and illustrate the importance of using spatially varying temperature changes for realistic climate simulations. In Fig. 3, the surface distribution of the temporally-averaged RCP 8.5 changes show that: for the atmosphere, the orography plays a major role in terms of the intensity of the changes (i.e. the strongest increase in temperature, decrease in relative humidity and change in wind speed are generally found at the highest altitudes), and, for the ocean, the changes imposed to the Adriatic and northern Ionian Seas (i.e. strongest increase in temperature and salinity) do not correspond to the changes imposed in the western side of the domain where the strongest changes in current speed occur. Concerning the sea surface elevation, the RCP 8.5 changes are mostly negative and only of the order of a few centimeters (with a maximum of 8 cm). Given that on the one hand, the open boundary of the LMDZ4-NEMOMED8 model (similarly to all the Med-CORDEX simulations, Adloff et al. 2018) does not properly include the projected Atlantic sea-level changes, but just takes into account the thermosteric effects and, on the other hand, the thermal stretching is balanced by the haline shrinking, these results are in accordance with the estimated –7 cm to 13 cm expected in the Mediterranean Sea (Tsimplis et al. 2008; Jordà and Gomis 2013; Gualdi et al. 2013). Thus, for realistic sea-level projections, mass change-induced sea-level increase—approximated to 50–60 cm in the Mediterranean till 2100 (Jordà and Gomis 2013), should be added to the presented PGW sea-level estimates.

In addition to the changes imposed to the ERA-I and MEDSEA forcing presented in the previous paragraphs, the volume mixing ratio of five atmospheric gases (carbon dioxide, methane, nitrous oxide and chlorofluorocarbons 11 and 12) used in the evaluation runs is modified in the scenario runs using projected values (Bernstein et al. 2008) averaged between 2060 and 2100 (Table 3). Further, the historical monthly Adriatic Sea river discharges are climatologically changed for the RCP 4.5 and RCP 8.5 scenarios (Fig. 4) following the study of Macias et al. (2018). Concerning the waves, the forcing used in the evaluation simulations were

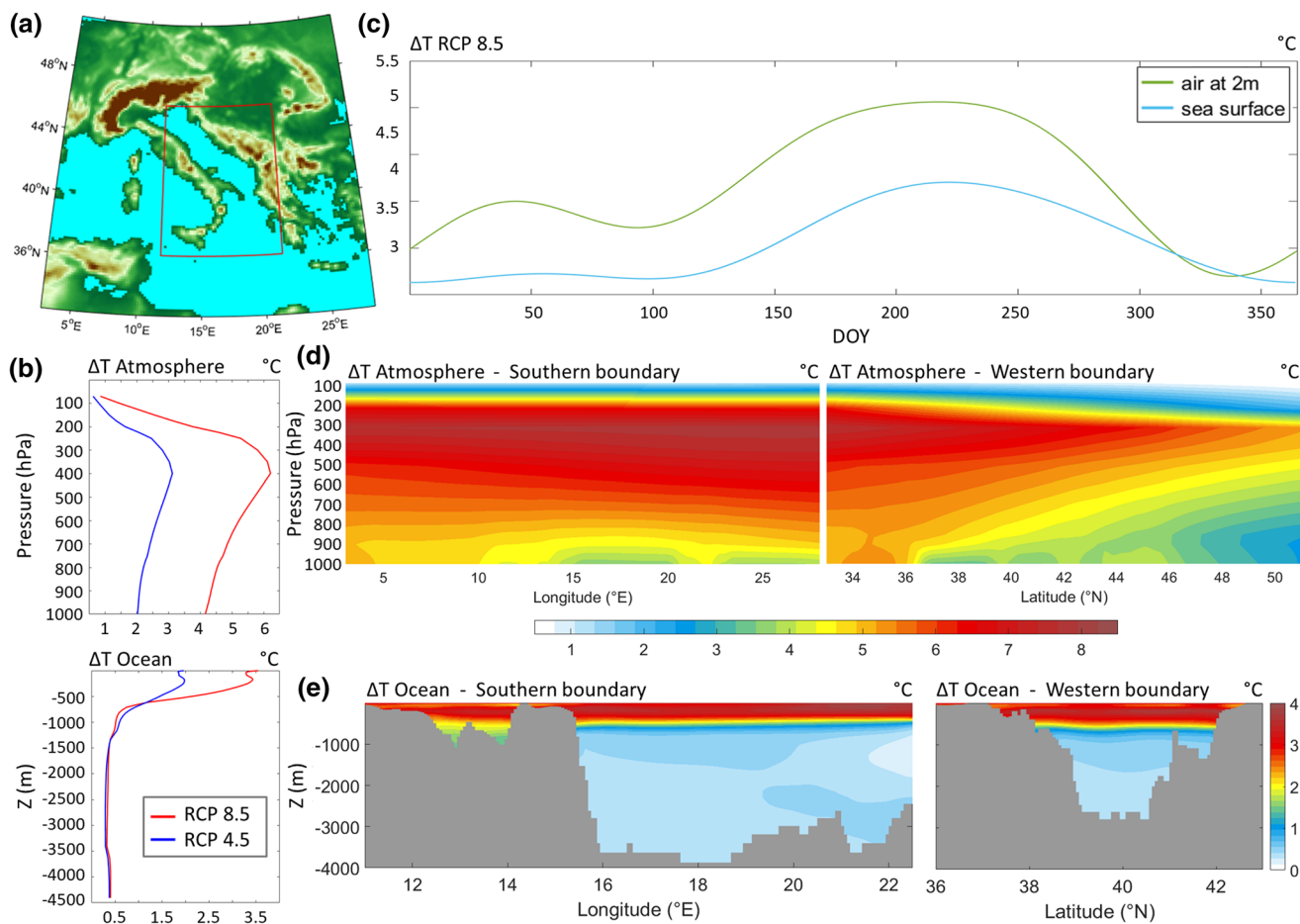


Fig. 2 **a** Spatial domain and boundaries of the WRF 15-km model and, within the red box, the ROMS 3-km model. **b** Vertical variations of the spatially- and temporally-averaged temperature changes ΔT for scenarios RCP 4.5 and RCP 8.5 following pressure level in the atmosphere and depth in the ocean. **c** Time evolution depending on the

day of a year (DOY) of the spatially-averaged 2-m air (in green) and sea-level (in blue) climatologic temperature changes ΔT for scenario RCP 8.5. Vertical structure of the temporally-averaged temperature changes ΔT (RCP 8.5) imposed at the southern and western boundaries of **d** the WRF 15-km model and **e** the ROMS 3-km model

kept unchanged for the scenario runs as the required data needed to apply the PGW methodology to the waves was not available. However, since the open boundary of the ROMS 3-km grid is located at least 400-km south of the Strait of Otranto, the wave field within the Adriatic basin is not considered to be highly affected by the propagation of these forcing. Finally, as this study aims to estimate the impact of climate change on atmospherically-driven extreme events and not to forecast future storms, the tidal forcing imposed for the evaluation runs was also kept unchanged for the scenario runs.

To summarize, the set of 108 runs used in this study consists in 36 Adriatic Sea wave storm simulations (selected in Sect. 2.2) carried out with the AdriSC modelling suite (described in Sect. 2.1)—for 3 days within the general module (i.e. coupled WRF-ROMS-SWAN) and 1.5 day within the nearshore module (i.e. WRF 1.5-km and coupled ADCIRC-unSWAN), in evaluation mode first and then

in climate change mode, for both RCP 4.5 and RCP 8.5 scenarios, imposing the PGW methodology (presented in Sect. 2.3).

3 Results

3.1 Evaluation of the AdriSC nearshore module wave component

To assess the skill of the AdriSC unSWAN model, the last 24-h of the 1-min significant wave height, peak wave period and mean wave direction results are extracted from the 36 simulations carried out in evaluation mode at the 11 locations of the wave stations presented in Sect. 2.2. The data are analyzed in three steps (see Figs. 5, 6, 7). First, the overall behavior of the model is presented as a scatter plot (Figs. 5a, 6a, 7a) for the entire set of simulations and measurements.

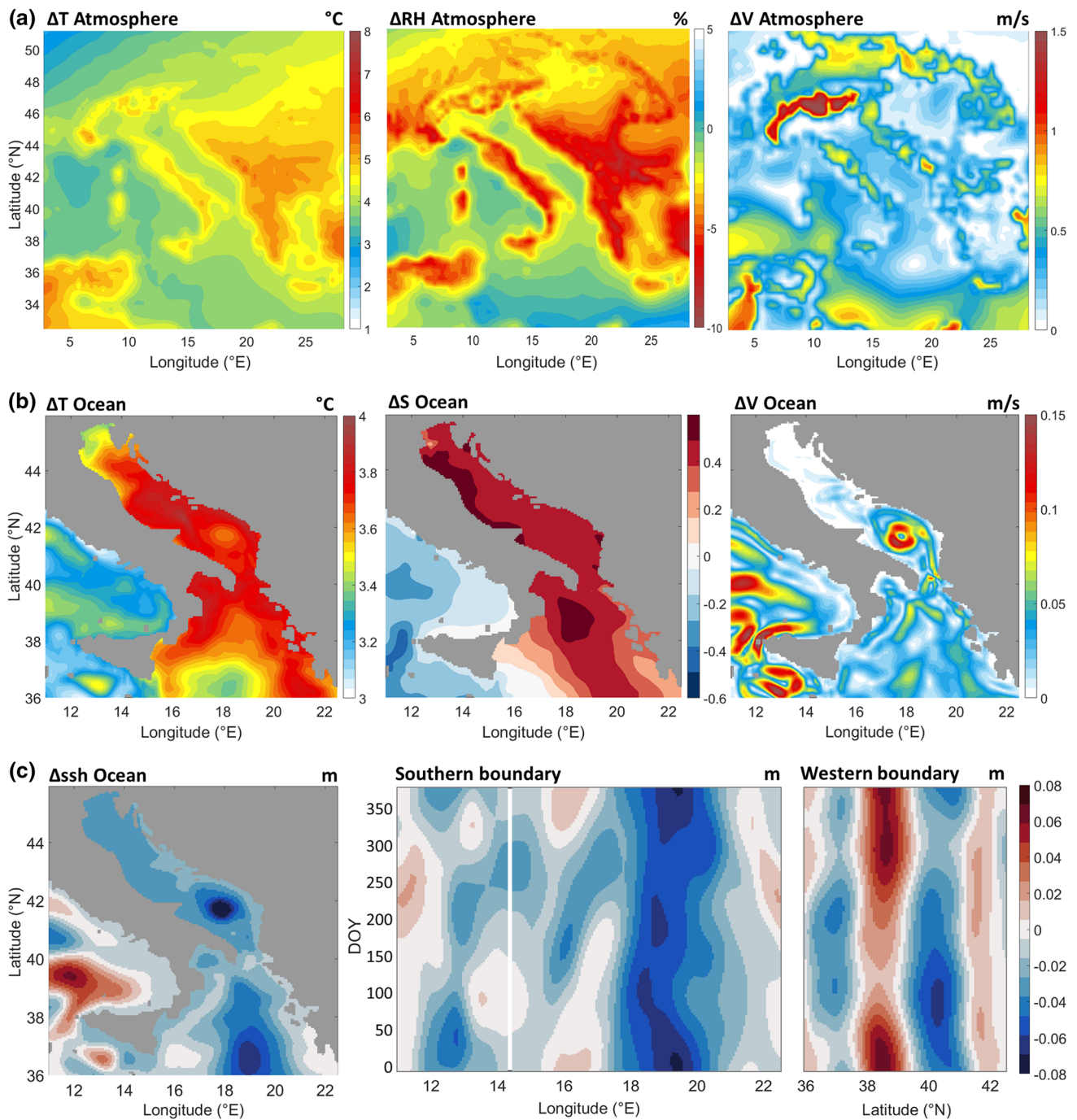


Fig. 3 Surface distribution of the temporally-averaged RCP 8.5 changes of **a** temperature (ΔT), relative humidity (ΔRH) and wind speed (ΔV) in the atmosphere for the WRF 15-km domain and **b** temperature (ΔT), salinity (ΔS) and current speed (ΔV) in the ocean for

the ROMS 3-km domain. The variations of the sea surface elevation (Δssh) RCP 8.5 changes are presented in **c** as temporally-averaged surface distributions and time-varying open boundary conditions

Then, the quantile–quantile distributions of the wave parameters are displayed separately for the Italian and Croatian wave stations (Figs. 5b, 6b, 7b) and, finally, the performance of the unSWAN model wave distributions during bora and sirocco events (Figs. 5c, 6c, 7c) is illustrated with violin plots (Hintze and Nelson 1998).

On the whole (Figs. 5, 6, 7), for the 36 studied storm events, the unSWAN model is in good agreement with the available wave measurements (significant height, peak period and mean direction): (1) in the scatter plots, the points with higher density (in red) are mostly located along the reference lines, (2) the quantile–quantile distributions for

Table 3 Atmospheric gas volume mixing ratios used for the evaluation and scenario runs

	Carbon dioxide CO ₂ (ppmv)	Methane CH ₄ (ppbv)	Nitrous oxide N ₂ O (ppbv)	Chlorofluorocarbon	
				CFC-11 (pptv)	CFC-12 (pptv)
Evaluation	379	1774	319	251	538
RCP 4.5	528	1680	365	105	242
RCP 8.5	762	3470	408	99	231

ppmv parts-per-million volume, ppbv parts-per-billion volume, pptv parts-per-trillion volume

Fig. 4 Monthly climatologic changes (in percentage) imposed to the Adriatic Sea river discharges for scenario runs RCP 4.5 and RCP 8.5

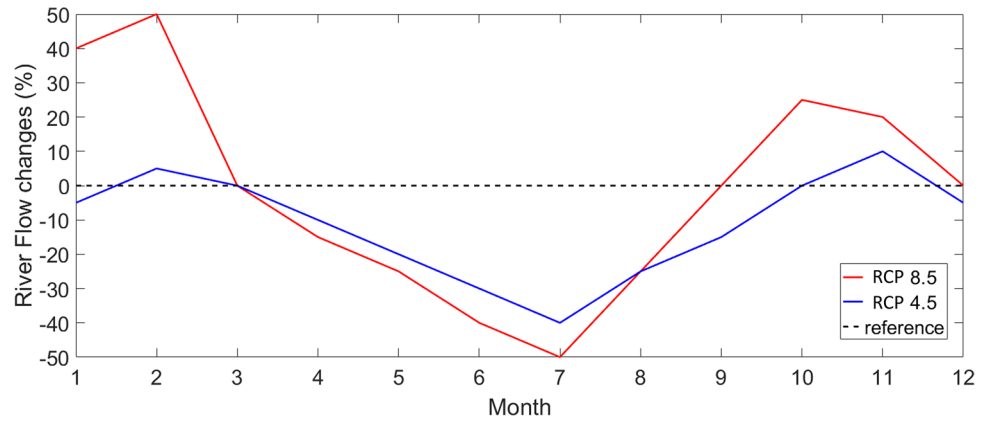


Fig. 5 Evaluation of the AdriSC unSWAN significant wave height distributions against measurements **a** for all the available stations and selected storm events as a scatter plot showing the density (number of occurrences #) with hexagonal bins, **b** separately for the Italian and Croatian stations as a quantile–quantile plot, and **c** separately for the bora and sirocco events as violin plot distributions

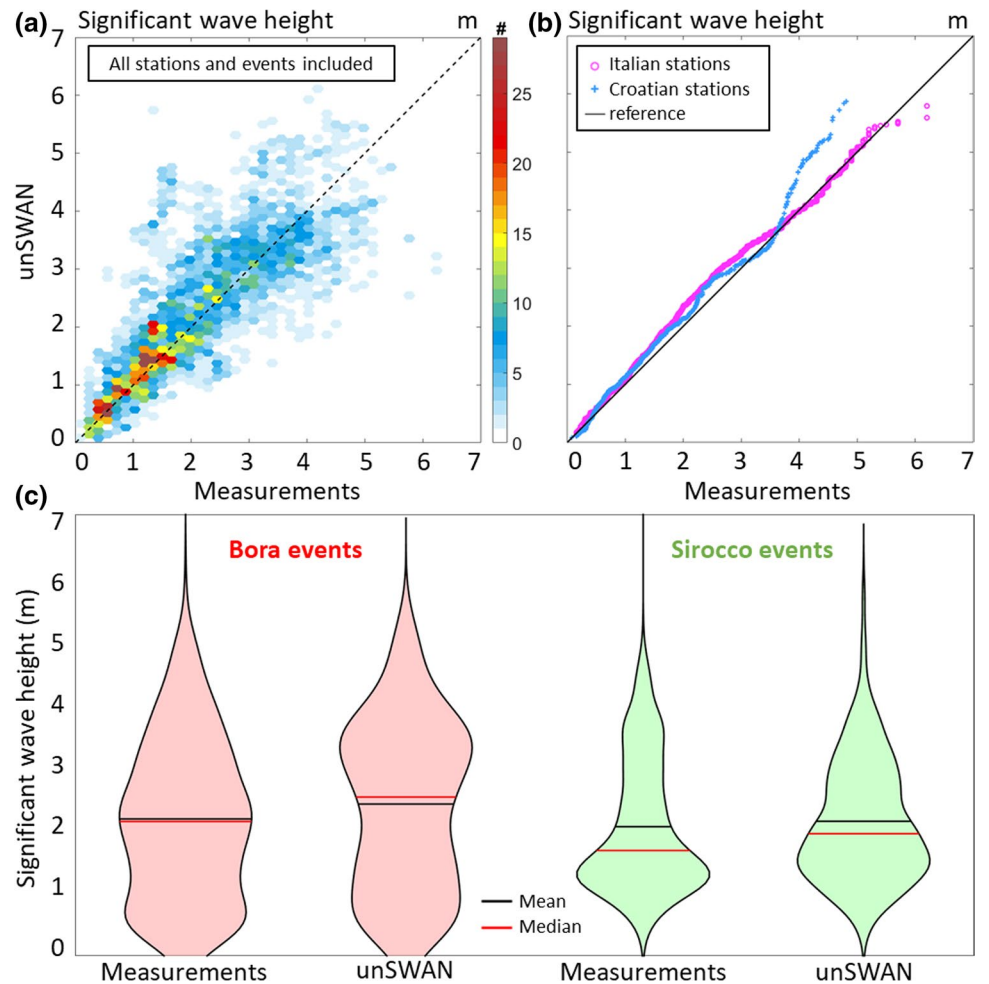
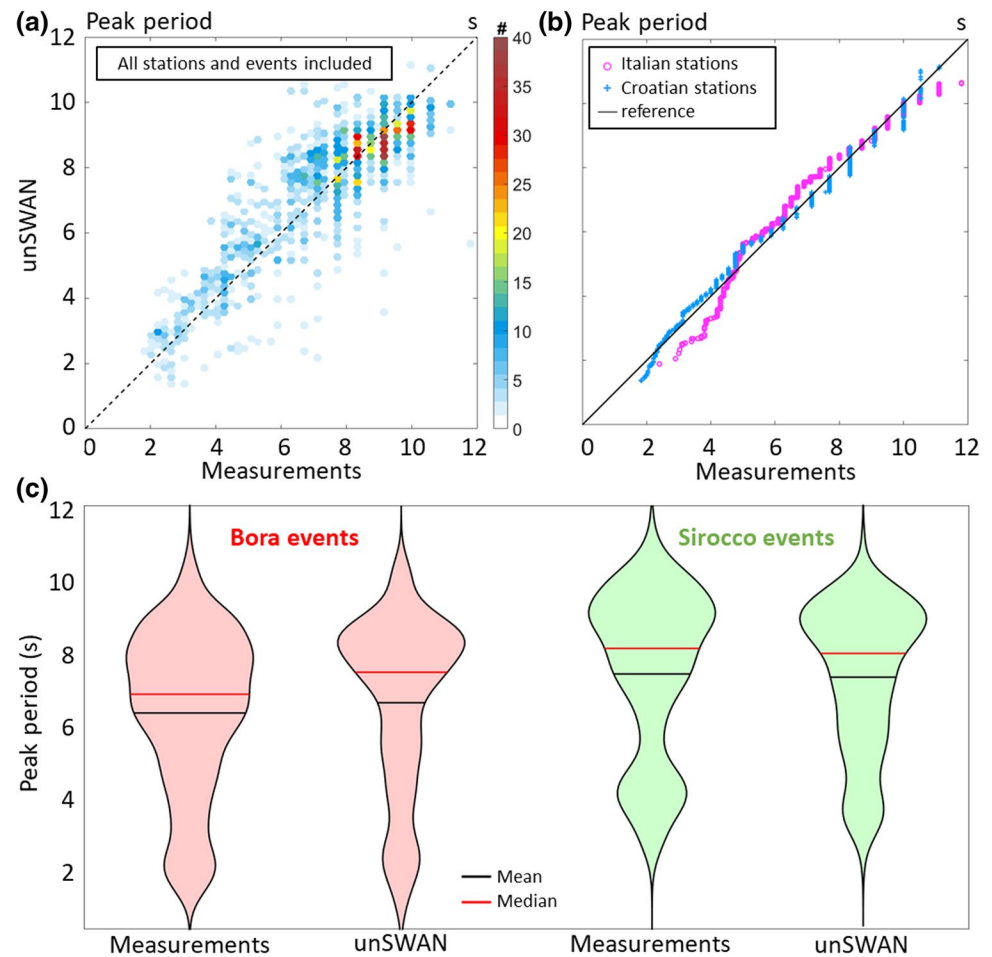


Fig. 6 As in Fig. 5, but for the peak wave period



both the Croatian and Italian stations also follow the reference lines, except for the mean direction which is not well reproduced for the Croatian stations, and (3) the shapes of the violin plots for the unSWAN model results are similar to those obtained for the measurements during both bora and sirocco events.

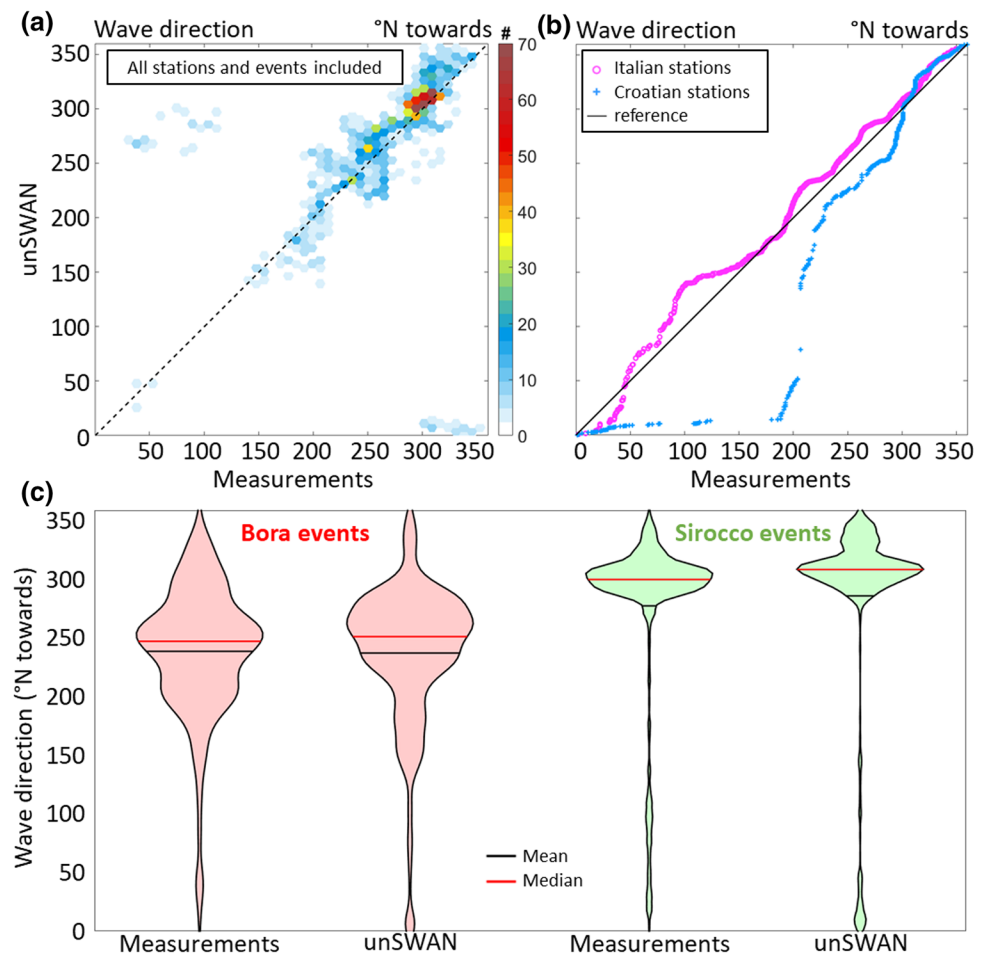
However, in more detail, some discrepancies between the measurements and the unSWAN model results can be noticed. For the significant wave height (Fig. 5), (1) the spread of the scatter plot (Fig. 5a) increases from about 0.25 m up to 2 m when reaching the highest values, (2) the model slightly overestimates (up to 0.25 m) the values between 2 and 4 m for both the Croatian and Italian stations and considerably overestimates (up to 1 m) the values above 4 m for the Croatian stations (Fig. 5b), and (3) the mean and median of the model distributions (Fig. 5c) are also overestimated for the bora (2.41 m vs. 2.17 m and 2.52 m vs. 2.13 m, respectively) and for the sirocco (2.13 m vs. 2.05 m and 1.94 m vs. 1.67 m, respectively) events.

For the peak wave period (Fig. 6), (1) similarly to the significant wave height, the spread of the scatter plot (Fig. 6a) increases from about 1 s up to 6 s when reaching the highest values (to be noted: the discontinuities seen in the plot

result from the fact that some measurements were provided as integer values), (2) the model slightly underestimates (up to 1 s) the values below 5 s and above 9 s for the Italian stations (Fig. 6b), and (3) the mean and median of the model distribution for the bora events (Fig. 6c) are overestimated (6.88 s vs. 6.61 s and 7.67 s vs. 7.10 s, respectively). Finally, for the mean wave direction, the major problem is the very large underestimation (up to 200°) of the values between 0° and 200° for the Croatian stations (Fig. 7b).

In a nutshell, the unSWAN model seems to have more difficulties to represent the wave conditions during bora events than during sirocco events, which means that the WRF 1.5-km model is most probably overestimating the intensity of the bora winds. Further, the model is capable of reproducing the intensity of the extreme wave events (see quantile–quantile distributions) but not their timing (see spread of the scatter plots), and have better agreement with measurements along the Italian coast than along the Croatian coast. For the last point, the analysis of each Croatian station (not shown here) reveals that the mismatching of the model for the wave directions between 0° and 200° principally occurs at the IVANA-A and Dubrovnik locations which, as the model is in good agreement with the data for the other

Fig. 7 As in Fig. 5, but for the mean wave direction



nine stations, likely results from a problem with the measurements at these two locations. Beside these limitations, the evaluation of the unSWAN model has shown that the newly added wave component of the AdriSC modelling suite can be used to reproduce the historical Adriatic wave storms with a good level of accuracy.

3.2 Impact of climate change on Adriatic extreme waves

With the aim to quantify the climate change impact on the Adriatic extreme wave events under both RCP 4.5 and RCP 8.5 projections for the 2060–2100 period, two kind of results are statistically analyzed: the spatial variations of the extreme wave conditions (Figs. 8, 9, 10), and the temporal variations of the wave parameters at chosen locations along the Adriatic Sea (Figs. 11, 12, 13, 14).

The spatial analysis of the extreme wave conditions consists first in defining the baseline conditions (Fig. 8), which are presented as the median over the ensembles of the 22 bora and the 14 sirocco storm simulations in evaluation (present climate) mode. The considered parameters are the maximum significant wave heights, maximum peak wave periods

and mean wave directions—calculated for each storm over the last 24-h results of the AdriSC nearshore module. Then, the climate change impact on the wave extremes is given by the differences (referred hereafter as climate adjustments) in maximum significant wave heights, maximum peak wave periods and mean wave directions between the climate change simulations (with the RCP 4.5 and RCP 8.5 scenarios treated separately) and the evaluation runs. Finally, the median and root-mean-square (RMS) of these climate adjustments are calculated for the ensembles of the 22 bora (Fig. 9) and the 14 sirocco (Fig. 10) events. The analysis of the baseline conditions (Fig. 8) shows that the typical significant wave heights and peak wave periods are above 3.5 m and 8 s, respectively. For the bora events, this particularly applies to the Italian coast between 42° N and 45° N of latitude, peaking between 44° N and 45° N latitude with the respective values of 5 m and 10 s. This is the result of the maximum in both bora speed and outreach, coming off the Croatian city of Senj at latitude 44.99° N (the Senj Jet, Grisogono and Belušić 2009). The typical wave propagation for the analyzed bora episodes is mostly towards south-west and west in the northern Adriatic and north-westward in the south. The latter indicates that majority of the selected

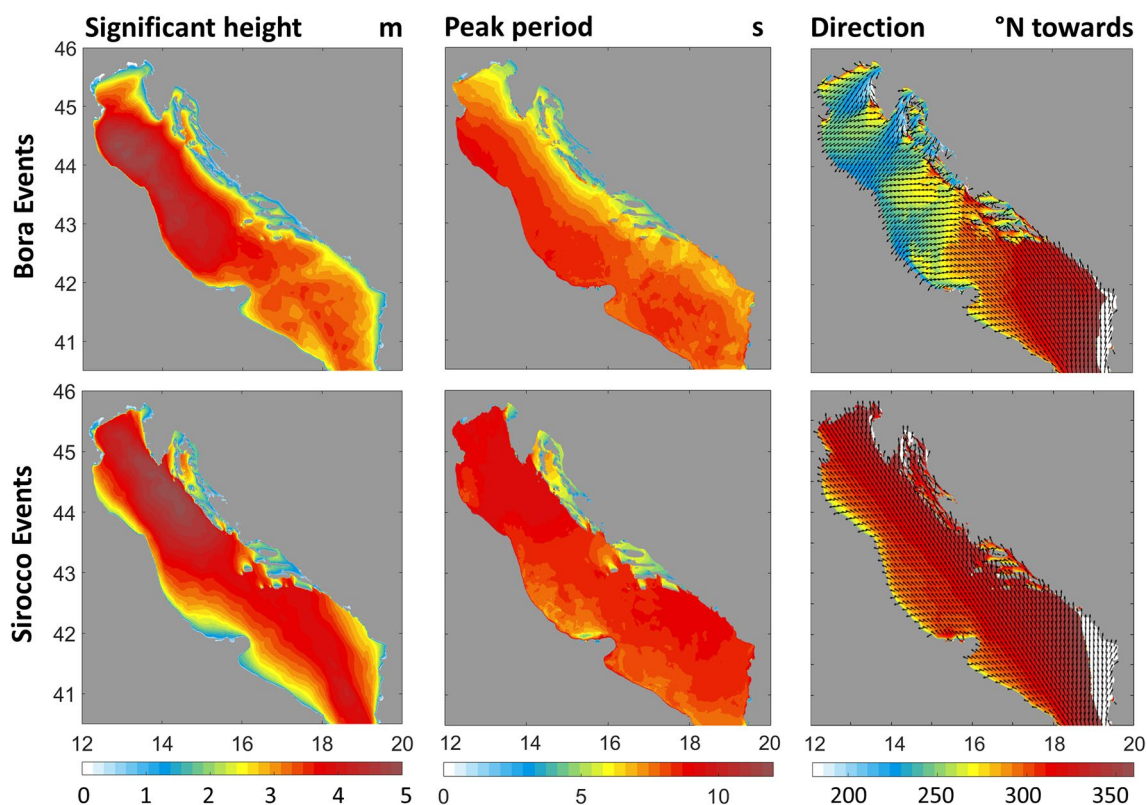


Fig. 8 Baseline (present climate) plots defined as the median, over the entire Adriatic Sea, of the maximum significant wave heights, the maximum peak wave periods and the mean wave directions of the 22 bora (top panels) and 14 sirocco (bottom panels) events

severe bora events peaked in the northern Adriatic, while being mostly conjoined with sirocco conditions in the southern Adriatic. For the sirocco events, wave heights are substantial in the open Adriatic Sea for the entire domain (except close to the Italian shoreline and in the coastal Croatian area), peaking with values up to 6 m associated with wave periods of 10 s between 44° N and 45° N latitude off the Croatian islands and coast. The typical wave propagation for sirocco events is towards north and north-west.

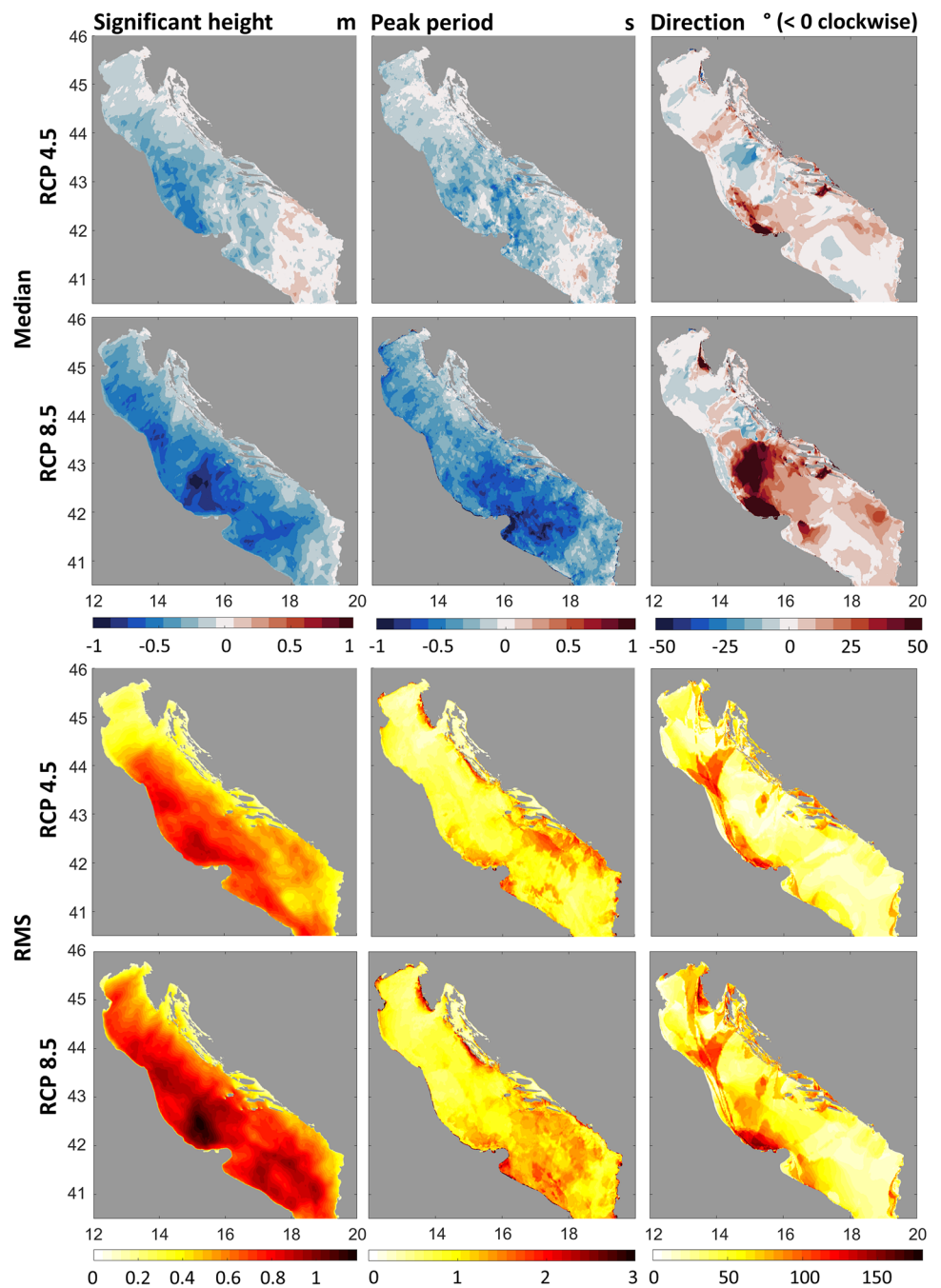
Typical significant wave heights and peak wave periods are foreseen, in the future climate, to overall decrease during bora events (Fig. 9), for both RCP 4.5 and RCP 8.5 scenarios. Negative median of the climate adjustment is projected over the entire Adriatic domain, except at its southern part in the RCP 4.5 scenario. For the RCP 8.5 scenario, the negative median of the climate adjustments reaches up to 1 m in significant height and 1 s in peak period off the Italian coast between 41°N and 43°N latitude and is associated with larger RMS values surpassing 0.8 m and 1 s, respectively. The direction of the bora winds is also affected over the entire domain (up to 50° change of direction for the RCP 8.5 scenario), but mostly along the Italian coastline between 42° N and 43° N latitude and regions where strong wind shear occur in the bora jets.

For the sirocco events (Fig. 10), the typical significant heights and peak periods are also mostly decreased in the northern Adriatic for both RCP 4.5 and RCP 8.5 scenarios (i.e. small or negative median of the climate adjustments) but increased (i.e. positive median of the climate adjustments) for the rest of the domain.

For the RCP 8.5 scenario, the northern Adriatic decreases can reach up to 0.5 m in significant height and 0.8 s in peak period and are associated with large RMS above 0.6 m and 0.5 s, respectively. Furthermore, the direction of the sirocco waves seems to be totally unchanged (both median and RMS of the climate adjustments are low) for both RCP 4.5 and RCP 8.5 scenarios.

The analysis of the temporal variations of the wave parameters during the selected Adriatic wave storms is based on the 1-min unSWAN series extracted at 5 open Adriatic Sea locations (O₁–O₅, Figs. 11, 12, 13, 14). A comparison between the distributions obtained in the evaluation and future climate (for RCP 4.5 and RCP 8.5 scenarios) simulations is performed, separately for the ensemble of the 22 bora and 14 sirocco events. The results are presented as a combination of scatter and probability density function (PDF) plots for the significant wave height and peak wave period parameters (Figs. 11, 12, 13),

Fig. 9 Climate change (RCP 4.5 and RCP 8.5) impact on the waves defined as the median and root-mean-square (RMS) of the climate adjustments (scenario minus evaluation results) of the maximum significant heights, the maximum peak periods and the mean wave directions of the 22 bora events



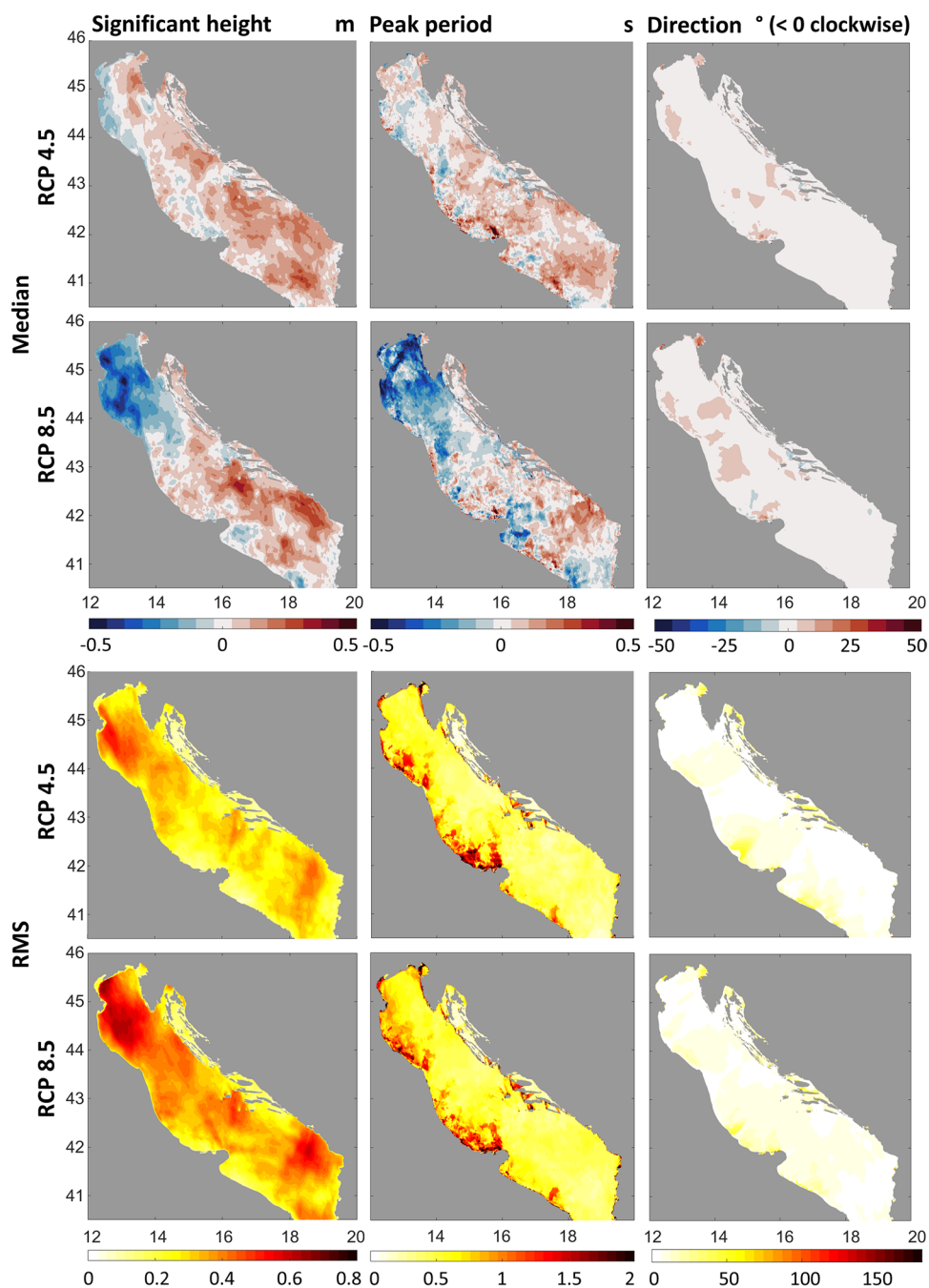
and as polar histogram plots for the mean wave direction (Figs. 12, 13, 14).

For the bora events (Figs. 11, 12), the scatter plots at the five chosen locations (Fig. 11) reveal that the overall distribution of the peak wave period vs. the significant wave height is not significantly modified under climate change projections and is presenting a strong linear relationship at all locations (i.e. the peak periods tend to increase linearly with the significant wave heights), with a little spread in the northern Adriatic only (locations O_4 and O_5). However, the analysis of the PDF distributions confirms that both peak

wave periods and significant wave heights during bora events are likely to decrease under climate change projections:

- concerning the significant wave height distributions, the values are consistently lowered in the future climate, with a minimum of 0.25 m at location O_5 (northern most part of the Adriatic Sea) for the RCP 4.5 scenario and a maximum of 2 m at location O_4 (where strongest bora wind are likely to blow) for the RCP 8.5 scenario while the tail is generally becoming less heavy under RCP 8.5 scenario at locations O_3 , O_4 and O_5 (i.e. the probability

Fig. 10 As in Fig. 9, but for the 14 sirocco events



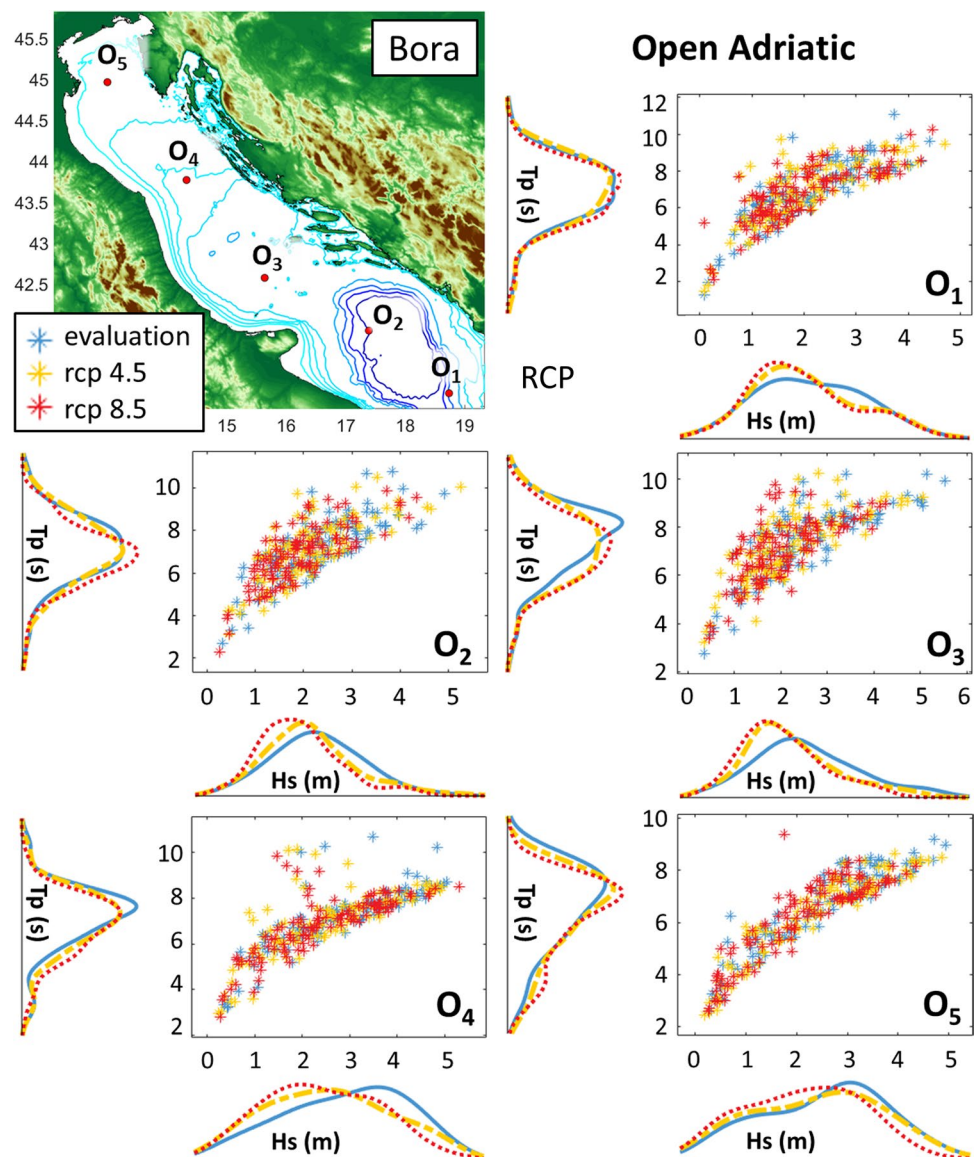
of significant wave heights above 3 m is largely reduced), but does not significantly change in the southern Adriatic (locations O_1 and O_2), at locations under the sirocco influence, for both RCP 4.5 and RCP 8.5 scenarios;

- concerning the peak wave period distributions, the values are also lowered at locations O_2 , O_3 , O_4 and O_5 , with a minimum of 0.5 s at location O_2 and a maximum of 1.5 s at location O_3 , both obtained for the RCP 4.5 scenario while, as for the significant wave height, the tail is generally becoming less heavy under RCP 8.5 scenario at all locations (i.e. the probability of the peak wave peri-

ods above 7 s is largely reduced), but does not present major changes for RCP 4.5 scenario, except at location O_5 (where the tail is clearly less heavy), and at location O_1 (where the tail is more heavy).

Regarding the mean wave direction distributions (Fig. 12), the most significant changes appeared at location O_3 where the waves primarily propagated westward in the evaluation mode, while they shift southward and south-eastward for both RCP 4.5 and RCP 8.5 scenarios. This behavior can also be noticed, in a smaller measure, at locations O_2 ,

Fig. 11 Peak wave period (T_p) vs. significant wave height (H_s) distributions derived from the 1-min AdriSC unSWAN evaluation and future climate projection (RCP 4.5 and RCP 8.5) results of the 22 bora events and extracted at 5 open Adriatic Sea locations (O_1 to O_5). The results are presented as a combination of scatter plots displaying the distributions of the peak period vs. the significant height



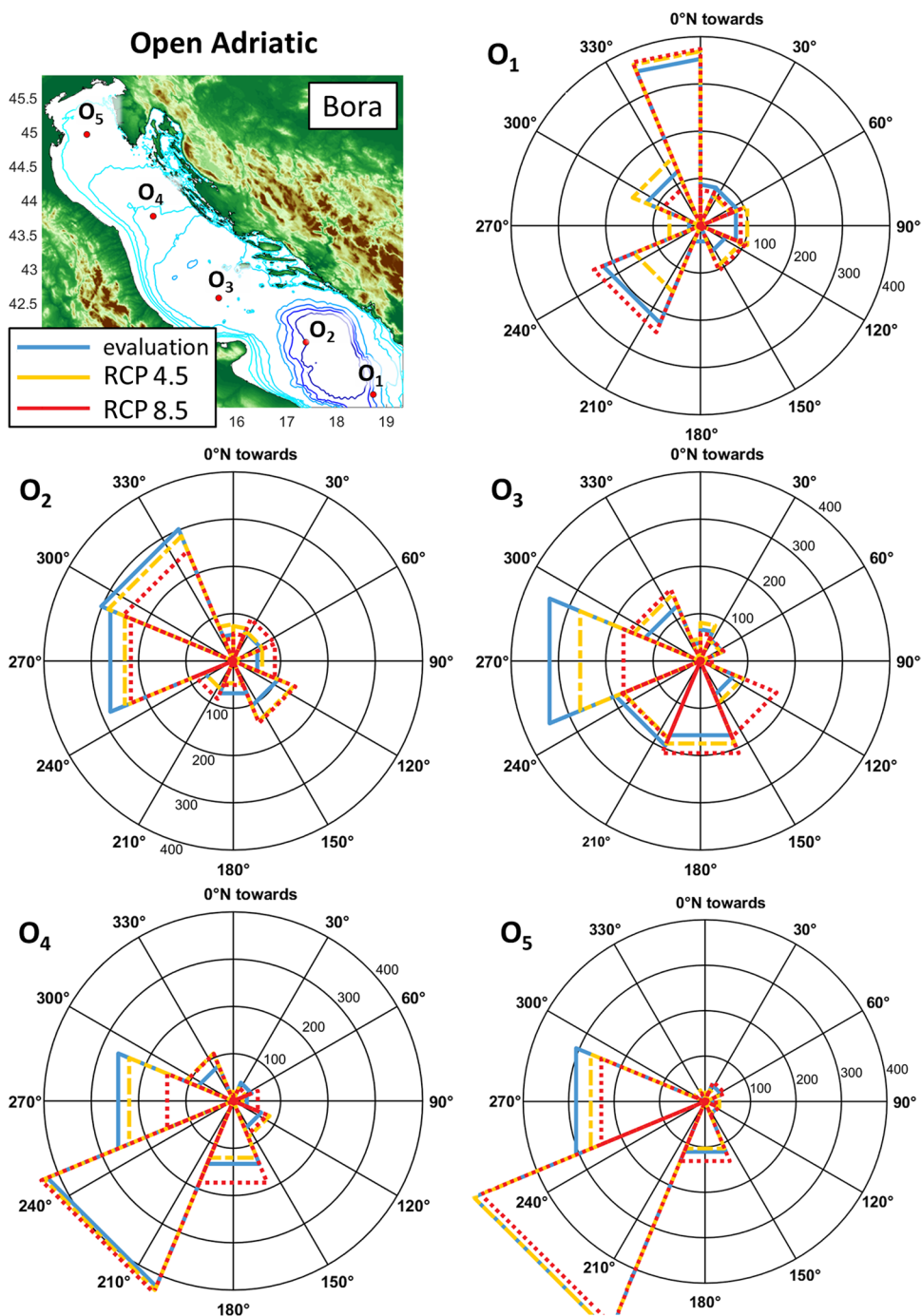
O_4 and O_5 (Fig. 12), where however the main direction of propagation is unchanged. Finally, at location O_1 , the most noticeable changes in direction occur for the RCP 4.5 scenario, where the south-westward waves are shifted to north-westward and south-eastward, but the main direction of propagation (i.e. north north-westward) is also unchanged.

For the sirocco events (Figs. 13, 14), as for the bora events, the scatter plots at the five chosen locations (Fig. 13) reveal that the overall distribution of the peak wave period vs. the significant wave height is not substantially modified under climate change projections. However, these distributions do not present a strong linear relationship in the northern Adriatic and show that, at locations O_3 , O_4 and O_5 , for peak periods above 7 s, significant wave heights can vary between 1 and 7 m. The analysis of the PDF distributions reveals that, compared to the bora events, less dramatic

changes are to be expected concerning the sirocco wave parameters under RCP 4.5 and RCP 8.5 scenarios:

- concerning the significant wave height distributions, the values are mostly unchanged, even though slightly (about 0.25 m in average) increased in the southern Adriatic Sea and decreased in the northern Adriatic Sea while the tail is, however, generally becoming less heavy under RCP 8.5 scenario in the northern Adriatic Sea at locations O_4 and O_5 (i.e. the probability of significant wave heights above 3 m is reduced) but slightly heavier or unchanged for the remaining locations under RCP 8.5 scenario and for all locations under RCP 4.5 scenario;
- concerning the peak wave period distributions, the values are also mostly unchanged at all locations and for both climate change scenarios, but the respective

Fig. 12 Mean wave direction distributions derived from the 1-min AdriSC unSWAN evaluation and climate projection (RCP 4.5 and RCP 8.5) results of the 22 bora events and presented as rose plots at 5 open Adriatic Sea locations (O_1 to O_5)



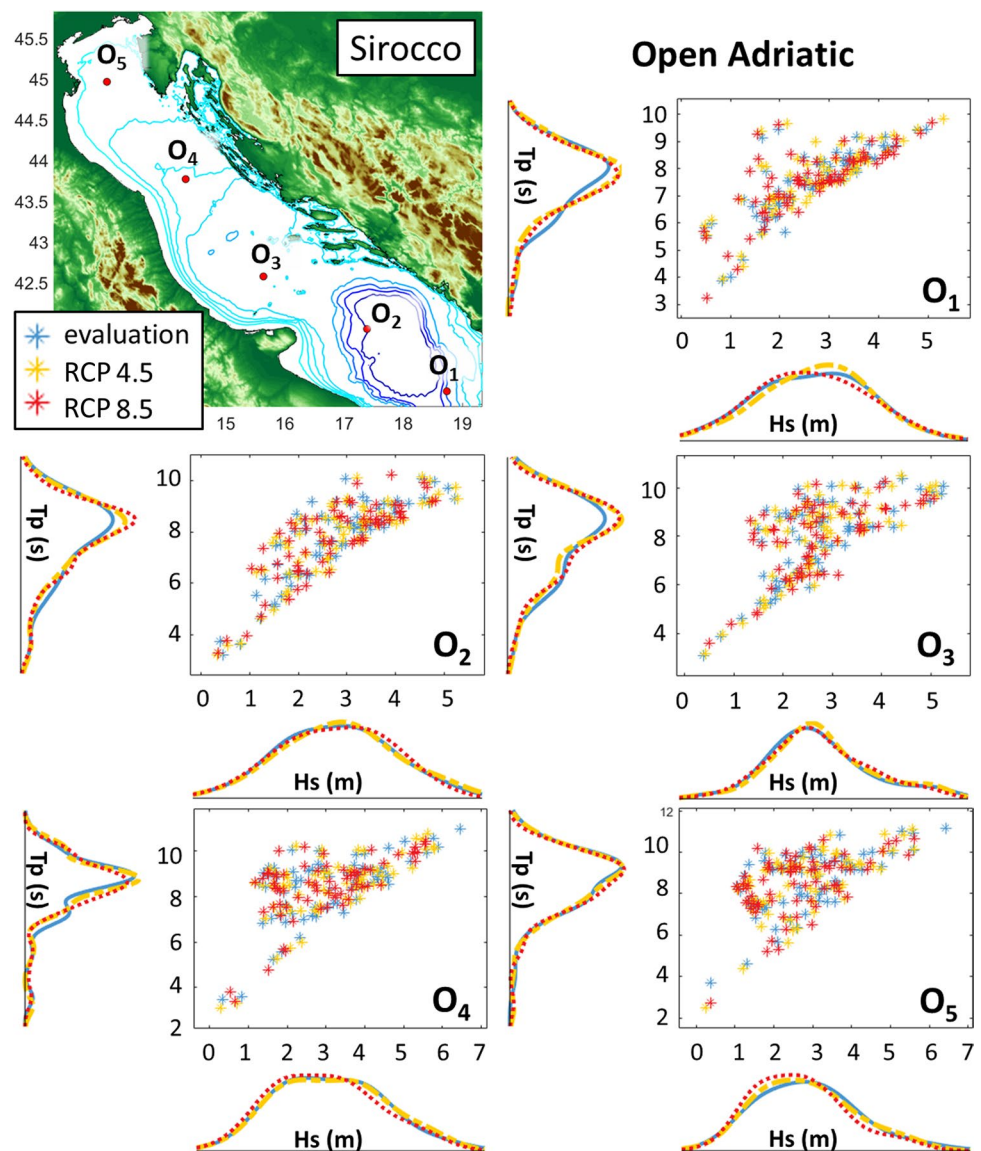
probabilities are increased in the southern Adriatic (locations O_1 , O_2 and O_3) while the tail is generally becoming slightly less heavy under RCP 8.5 scenario in the northern Adriatic (i.e. the probability of the peak wave periods above 9 s is reduced) but does not present major changes for RCP 4.5 scenario.

Finally, the mean wave direction distributions (Fig. 14) show that the north-westward main direction of the waves

in evaluation mode remains unchanged under both RCP 4.5 and RCP 8.5 scenarios.

To summarize, the spatial variations of the extremes and the 1-min time series—extracted along the open Adriatic Sea, reveal that, under warming climate change (for both RCP 4.5 and RCP 8.5 scenarios), significant wave heights and peak wave periods are likely to, on the one hand, strongly decrease over the entire domain with a south-eastward shift of direction in the central Adriatic during the

Fig. 13 As in Fig. 11, but for the 14 sirocco events



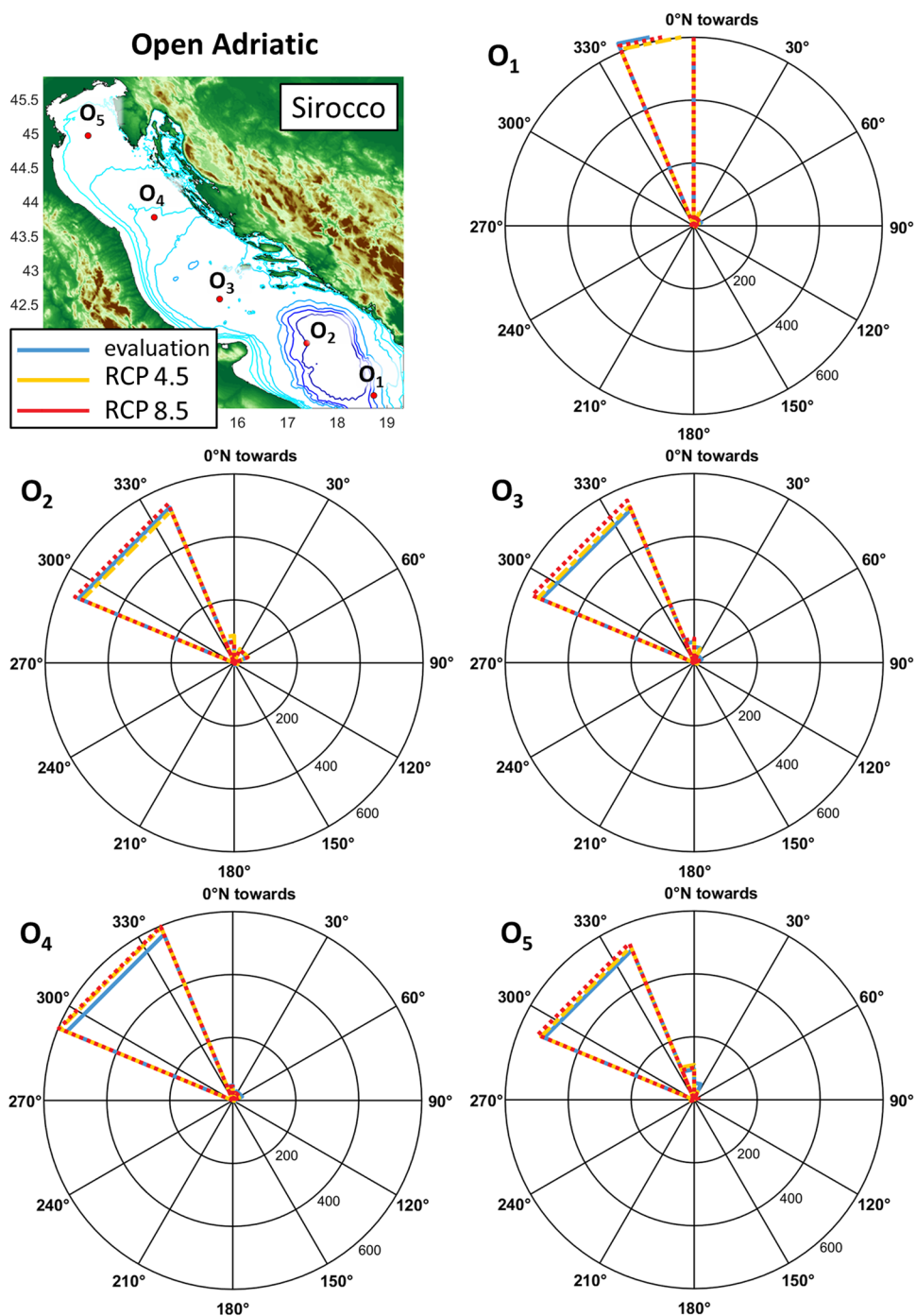
extreme bora events, and, on the other hand, decrease in the northern Adriatic with no significant change in direction during the extreme sirocco events. These results are in good agreement with the study of Belušić Vozila et al. (2019) who estimated the possible future changes in wind speed over the Adriatic region, for the 2041–2070 period, from an ensemble of 19 high-resolution (0.11°) CORDEX simulations and found that overall the mean wind speed as well as the number of storms is reduced under the RCP 8.5 scenario for both bora and sirocco conditions. However, Belušić Vozila et al. (2019) also highlights an increase of the bora mean wind speed in the northern Adriatic, which is not in accordance with the presented results (Figs. 9, 11). Although selection of bora events differs between the two studies, this result may indicate the limitation of the PGW methodology which can only be used to assess how past storms would behave under climate change. Additionally, the

presented results are in good agreement with other wave climate studies, which all envisage a decrease of wave heights in the Adriatic Sea, in particular concerning sirocco events (Benetazzo et al. 2012; Lionello et al. 2012a; Bonaldo et al. 2017; Pomaro et al. 2017).

3.3 Impact of climate change on northern Adriatic storm surges

In terms of the climate change impact on storm surges, the flooding of the coastal cities along the Adriatic coast—and most particularly in the northern Adriatic, is known to be driven by extreme sirocco conditions (e.g. Robinson et al. 1973; Cavaleri 2000; Cavaleri et al. 2010; Raichich 2015; Medugorac et al. 2015), such as those selected in Sect. 2.2 which led to the highest water levels recorded in Venice lagoon between 1979 and 2019. The atmospherically-driven

Fig. 14 As in Fig. 12, but for the 14 sirocco events

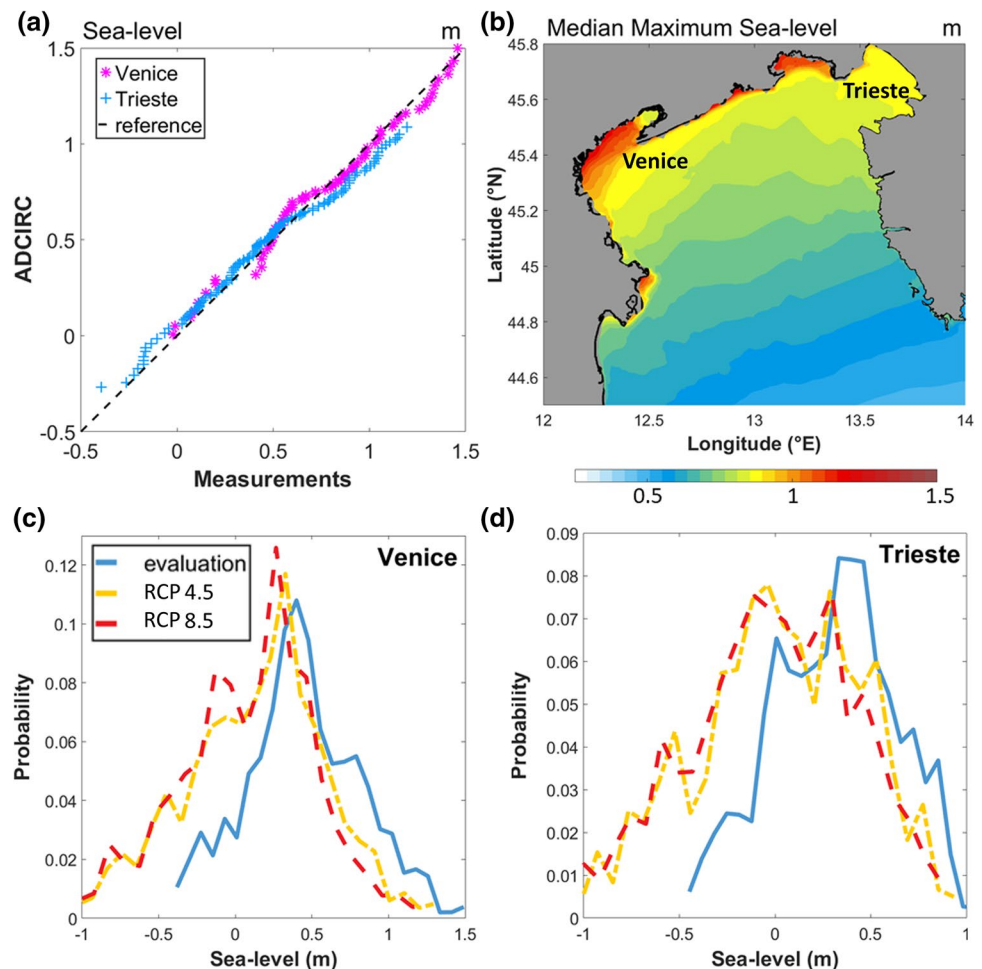


extreme sea-level changes in the northern Adriatic under RCP 4.5 and RCP 8.5 scenarios and following the PGW methodology can thus be assessed in this study with the ensemble of the selected 14 sirocco events.

The AdriSC ADCIRC model capability to reproduce the storm surges in the northern Adriatic and more specifically in the Venice Lagoon and the Gulf of Trieste is first assessed with a sea-level distribution quantile–quantile analysis (Fig. 15a) of the available hourly measurements and

the ADCIRC model results—extracted at the locations of the two tide gauges (Sect. 2.2) from the last 24-h results of the 14 sirocco simulations carried out in evaluation mode. To be noted, (1) as the bathymetry used in the ADCIRC model may be imprecise and may use a different vertical reference level than the tide gauges, the local mean sea-levels of the model results at Venice and Trieste locations were adjusted by adding the difference between the measured and the modelled mean values calculated for the ensemble of

Fig. 15 Analysis of the northern Adriatic storm surge distributions during the 14 sirocco events: **a** quantile–quantile analysis of the AdriSC ADCIRC results and the measurements at Venice and Trieste tide-gauge stations, **b** baseline sea-level plot defined as the median of the maximum sea-levels generated by each storm, **c, d** sea-level distributions derived from the 1-min AdriSC ADCIRC evaluation and climate projection (RCP 4.5 and RCP 8.5) results and extracted respectively at Venice and Trieste tide gauge stations



the 14 sirocco events; (2) as tides play an important role on extreme storm surges, they were not removed from the sea-level signals, and (3) as this study only aims to present the climate change impact on the sea-level distributions during sirocco events in the northern Adriatic Sea and not to reproduce individual storm surges, the model evaluation can be performed with the presented quantile–quantile analysis.

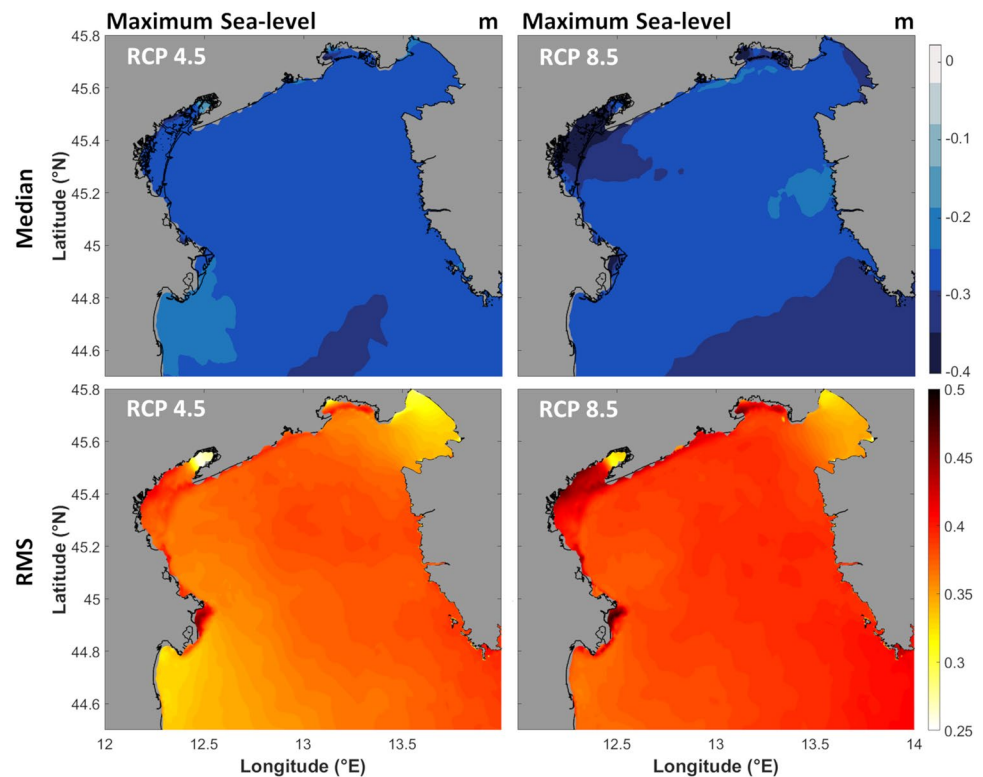
Similarly to the analysis performed for the waves in Sect. 3.2, the impact of climate change for the 2060–2100 period on the northern Adriatic storm surges under both RCP 4.5 and RCP 8.5 projections, is then estimated via the statistical analysis of two kind of results: the spatial variations of the maximum sea-levels obtained for each storm (Figs. 15b, 16) and the 1-min sea-level temporal variations at both the Venice Lagoon and the Gulf of Trieste tide gauge locations (Fig. 15c, d).

For the spatial variations, the sea-level baseline condition (Fig. 15b) is defined as the median over the ensemble of the 14 selected storm simulations in evaluation mode and their maximum sea-levels—calculated for each storm over the last 24-h results of the AdriSC nearshore module. As in Sect. 3.2, the climate change impact on the storm surges

is given by the differences (referred hereafter as climate adjustments) in maximum sea-levels between the climate change simulations (with the RCP 4.5 and RCP 8.5 scenarios treated separately) and the evaluation runs. The median and root-mean-square (RMS) of these climate adjustments are calculated for the ensemble of 14 sirocco events (Fig. 16). In terms of the results, the baseline condition (Fig. 15b) shows that typical storm surges during sirocco events reach 1.4 m in the Venice Lagoon and 0.9 m in the Gulf of Trieste and, under climate change conditions (Fig. 16), are decreased (i.e. negative median of the climate adjustments) by more than 0.25 m over the entire northern Adriatic domain for both RCP 4.5 and RCP 8.5 scenarios, and by more than 0.35 m in the Venice Lagoon for the RCP 8.5 scenario. The decrease of the storm surges in the future climate is also associated with an important variability (i.e. RMS) of about 0.35 m in average for both RCP 4.5 and RCP 8.5 scenarios and reaching more than 0.45 m in the Venice Lagoon for RCP 8.5 scenario.

These results are confirmed by the temporal analysis of the sea-level distributions (for the evaluation runs and the RCP 4.5 and RCP 8.5 projections) at Venice and Trieste

Fig. 16 Climate change (RCP 4.5 and RCP 8.5) impact on the northern Adriatic extreme sea-levels defined as the median and root-mean-square (RMS) of the climate adjustments (scenario minus evaluation results) of the maximum sea-levels for the 14 sirocco events



tide gauge locations (Fig. 15c, d). It appears that, at both locations under RCP 4.5 and RCP 8.5 climate change, the modes of the sea-level distributions are decreased by about 0.25 m while the tails of the distributions are less heavy (i.e. the probability of storm surges above 0.75 m is greatly decreased) and the maximum surges are reduced by about 0.25 m. Finally, the probability of sea-levels below -0.5 m (which was the minimum reached in evaluation mode) is largely increased which reveals that, under the climate change projections, some of the strong sirocco events simulated in evaluation mode might take more time to develop (or never developed) as storms of lower intensity in the RCP 4.5 and RCP 8.5 simulations. Thus, for these events, the wind-wave set-up—building up in the northern Adriatic during the 3 days of simulation in evaluation mode, was decreased as it built up over a smaller period with weaker winds (or did not built up at all).

To summarize, under climate change projections with imposed PGW methodology, the northern Adriatic sirocco storm surges are not only likely to decrease but also to be less frequent, which is in accordance with the analysis of the sirocco wind and storm surge projections (Lionello et al. 2012a; Androulidakis et al. 2015; Belušić Vozila et al. 2019). However, as the subsidence of the Venice Lagoon is not considered in this study, and the sea-level change is imposed as a mean effect for the entire 2060–2100 period in the PGW methodology ignoring the Atlantic global sea-level rise (see discussion about sea surface elevation in Sect. 2.3),

these results do not imply that flooding of the Venice city will be less likely in the future.

4 Discussion and conclusions

Understanding how climate change could impact extreme wave storms—one of the most devastating natural hazards occurring along the littoral, is of crucial importance for the future of coastal communities. However, in order to properly capture such atmospherically-driven extreme events and their repercussions on the coast (e.g. extreme wave and storm surges, coastal erosion, etc.), the implementation of computationally expansive kilometer-scale coupled ocean–wave–atmosphere models is required for each specific coastal region considered. Consequently, the classical approach used in climate studies (i.e. 30 years of evaluation run, 50 years of historical run and 100 years of scenario runs) is too impractical and costly to be applied for this kind of investigations. As an alternative, the pseudo-global warming (PGW) methodology—originally developed for kilometer-scale atmospheric studies, presents the advantage of generating at a limited computational cost (i.e. once the PGW climatological forcing is created, each event can be simulated over a short period of time) an ensemble of storms used to statistically assess the impact of climate change on extreme events.

The principal novelty of this study was thus to implement the PGW method within the AdriSC modelling suite—a multi-model chain dedicated to the study of the Adriatic Sea (Denamiel et al. 2019), which couples the atmospheric model WRF at 15-km, 3-km and 1.5-km of resolution with the ocean and wave models ROMS and SWAN at 3-km and 1-km of resolution and the unstructured ADCIRC and SWAN models with up to 10 m resolution along the coast. In particular, a lot of attention was paid to the best way to represent not only the ocean forcing (salinity, temperature, currents) but also the sea-levels, the rivers, the waves and the tides. As the Adriatic Sea collects up to a third of the Mediterranean Sea fresh water budget (Ludwig et al. 2009), the river discharge forcing—which is projected to be highly impacted by climate change, was modified following the study of Macias et al. (2018). However, due to the known uncertainties and/or lack of data linked to sea-level rise and wave climate projections over the entire Mediterranean Sea (Ruti et al. 2016; Adloff et al. 2018), these forcing were kept unchanged in this work. Additionally, in order to only account for the impact of global warming in the storm surge analysis, the tidal forcing also remained untouched. If these approximations have little consequences on the extreme wave results (as the boundary of the SWAN 3-km model is far enough from the studied area), they can impact the presented storm surge distributions due to the non-linear nature of their interactions with the nearshore water depths—including local sea-levels and tides (Johns et al. 1985; Speer and Aubrey 1985; Parker 1991; Zhang et al. 2017; Yang et al. 2019). The impact of sea-level rise was thus ignored in this work and only the atmospherically-driven storm surge distributions were analyzed.

The other important component of this numerical work was to provide a thorough evaluation of the AdriSC modelling suite skill to reproduce historical extreme events and to provide meaningful climate projections via the PGW method. To achieve these goals an ensemble of 22 bora and 14 sirocco extreme wind-wave events were selected between 1979 and 2019 and ran in both evaluation and climate projection (for RCP 4.5 and RCP 8.5 scenarios) modes. The evaluation of the distributions of both the wave parameters (significant height, peak period and mean direction) against 11 stations located along the Adriatic coast, and the storm surges against the Venice and Trieste tide gauges, revealed that overall the AdriSC model is capable of reproducing the selected 36 historical extreme events. Concerning the climate simulations with the PGW method, the wave and storm surge distributions—showing a general decrease of the extreme bora and sirocco intensity for both RCP 4.5 and RCP 8.5 scenarios, follow the previous studies published in the Adriatic Sea (Benetazzo et al. 2012; Lionello et al. 2012a; Androulidakis et al. 2015; Bonaldo et al. 2017; Pomaro et al. 2017; Belušić Vozila et al. 2019) and thus

the statistical approach consisting in running ensembles of short simulations for extreme events seems to provide robust results. However, it should be noticed that, (1) as only a small ensemble of storms was selected, the simulated wave and storm surge distributions may not be fully representative of neither the historical Adriatic extreme events between 1979 and 2019 nor their future projections for the 2060–2100 period, (2) as the simulations were performed over a three-day period, the last 24-h results analyzed in this study might be influenced by the imposed initial conditions and finally, (3) as the same ensemble of storms is used in evaluation and climate projection modes, the frequency of the extreme events cannot be analyzed with the PGW method. Additionally, due to the lack of reliable ocean–atmosphere Med-CORDEX runs at the time of this study, the climatological forcing used in the presented PGW simulations were derived from a single model instead of an ensemble of Regional Climate Models (RCMs) which would have provide more robust climate change projections. The generation of such a forcing, or potentially of an ensemble of PGW simulations—as already adopted by the atmospheric community (e.g. Li et al. 2019), could be achieved in a near future when more ocean–atmosphere RCMs will become available in the Mediterranean Sea.

Notwithstanding the limitations of the PGW approach implemented in the AdriSC modelling suite, this study demonstrates that such a method has the potential to be applied to kilometer-scale ocean–atmosphere models for long- or short-term simulations which can be embedded in the traditional CORDEX sub-domains including an oceanic component (e.g. Ruti et al. 2016; Tinker et al. 2016; Zou and Zhou 2016; Han et al. 2019). For coastal areas such as the Adriatic Sea, this can open the door to a better understanding of the climate change impacts on various processes (e.g. dense water formation, ocean sea surface thermal interactions during storms and hurricanes, etc.) closely depending on the air–sea feedback mechanism.

Acknowledgements The contribution of all the organisations that kindly provided the observations used in this study—Copernicus Marine Environment Monitoring Service, data buoy network of the Istituto Superiore per la Protezione e la Ricerca Ambientale (ISPRA, Italy), Hrvatski hidrografski institut (HHI, Croatia) and Istituto di Scienze Marine (ISMAR, Italy), is acknowledged. Special thanks to Roman Brogli from the Eidgenössische Technische Hochschule (ETH Zürich, Switzerland), Laurent Li from the Université Pierre et Marie Curie (Paris, France) and Srđan Čupić from HHI (Croatia) who provided respectively insights concerning the pseudo-global warming (PGW) method, the regional climate model ocean–atmosphere results (from LMDZ4-NEMOMED8) used in this study and the wave measurements along the Croatian coastline. Acknowledgement is also made for the support of the European Centre for Middle-range Weather Forecast (ECMWF) staff, in particular Xavier Abellan and Carsten Maass, as well as for ECMWF's computing and archive facilities used in this research. Finally, the authors would like to thank the two anonymous reviewers for their valuable comments. This work has been supported

by projects ADIOS (Croatian Science Foundation Grant IP-2016-06-1955) and ECMWF Special Project (The Adriatic decadal and inter-annual oscillations: modelling component).

Author contributions IV and CD contributed to the study conception and design. Material preparation and data collection were done by HM and CD. Set-up of the models and simulations were performed by FQ and CD. Analysis of the results and production of the figures were performed by PP, IV and CD. The first draft of the manuscript was written by CD and all authors commented on previous versions of the manuscript. All authors read and approved the final manuscript.

Funding ADIOS project: Croatian Science Foundation Grant IP-2016-06-1955. European Centre for Middle-range Weather Forecast (ECMWF) Special Project: The Adriatic decadal and inter-annual oscillations: modelling component).

Availability of data and material The model results and the measurements used to produce this article can be obtained under the Open Science Framework (OSF) FAIR data repository <https://osf.io/7d6jq/> (<https://doi.org/10.17605/osf.io/7d6jq>).

Code availability Codes used to produce this article can be obtained under the Open Science Framework (OSF) FAIR data repository <https://osf.io/7d6jq/> (<https://doi.org/10.17605/osf.io/7d6jq>).

Compliance with ethical standards

Conflict of interest The authors declare that they have no conflict of interest.

Appendix 1

Despite an in-depth sensitivity study of the model resolution impact on extreme event representation being out of scope of this paper, the reasons why kilometer-scale resolution in the atmosphere and meter-scale resolution in the ocean are a pre-requisite to meaningful wave storm modelling in the Adriatic region are briefly discussed hereafter.

The first argument is based on recently published studies supporting the idea that Adriatic extreme events can only be captured with resolutions higher than those generally used in Regional Climate Models (RCMs). For the atmosphere, the capability of climate models to reproduce mesoscale wind phenomena has been tested and atmospheric resolution—via a better reproduction of the orography and consequently the enhancement of jet flows on finer grids, has been found to be one of the most important model characteristics known to impact wind speed driving extreme waves and storm surges in the Adriatic region (e.g. Belušić et al. 2017; Josipović et al. 2018). Similarly, for the ocean, extreme wave or flood hazard assessments have been found to only be achieved with models capable to reproduce the proper geomorphology (including complex coastline and bathymetry) of the Adriatic Sea coastal regions (e.g. Cavaleri et al. 2010, 2019; Torresan et al. 2019). Finally, based on the results of this

study, the quantile–quantile plots (Fig. 17) displaying the performance of the unSWAN and SWAN 1-km models for an ensemble of 11 stations and 36 extreme events (presented in Sect. 2) illustrate the impact of the model resolution on the significant wave height and peak wave period. They show that for extreme conditions the unSWAN model provides better results than the SWAN 1-km model, particularly concerning the peak wave period, even though wave heights are slightly overestimated by the unSWAN model and perfectly represented by the SWAN 1-km between 1 and 3 m.

The second argument presented here is that the inclusion of the precise coastline and bathymetry (e.g. the precise geomorphology of the Venice Lagoon) as well as the numerous small islands (more than 1000 islands, isles, islets, rocks are identified along the Croatian coast) acting as barriers during extreme storm events, is crucial to properly simulate wave transformation and consequently storm surges in the northern Adriatic. This geomorphological impact is illustrated (Fig. 17) with spatial plots of maximum significant wave height and maximum peak wave period for the unSWAN model and for the difference between the unSWAN and SWAN 1-km models during the sirocco storm of the 22nd of December 1979 and the extreme bora event of the 7th of February 2012. The effect of the geomorphology and the islands located along the eastern Adriatic Sea on the wave propagation and transformation is particularly seen on the unSWAN results which show that both maximum significant wave height and maximum peak wave period are smaller along the Croatian coasts than in the rest of the domain. The difference plots highlight that, on the one hand, the overall increase in maximum significant wave heights in the unSWAN simulations (between 0.5 and 1.5 m compared to SWAN 1-km) mostly results from the increase in resolution (and thus in intensity) of the atmospheric wind forcing and, on the other hand, for the presented bora event, the proper representation of the islands in the unSWAN simulations dramatically influenced the reproduction of the maximum peak periods (up to 5 s difference with the SWAN 1-km model).

Finally, the use of unstructured meshes is not only useful for pure oceanographic purposes but also for the study of other processes driven by extreme events such as, for example, the motion of boulders during sirocco storms which requires to perfectly reproduce the wave transformation at a meter-scale resolution to derive the transport of these blocks weighting up to a ton (see Biolchi et al. 2019b).

Appendix 2

As no catalogue of extreme historical bora events exists in the Adriatic region, an in-depth bibliographical research—presented in Table 4 and including meteorological bulletins

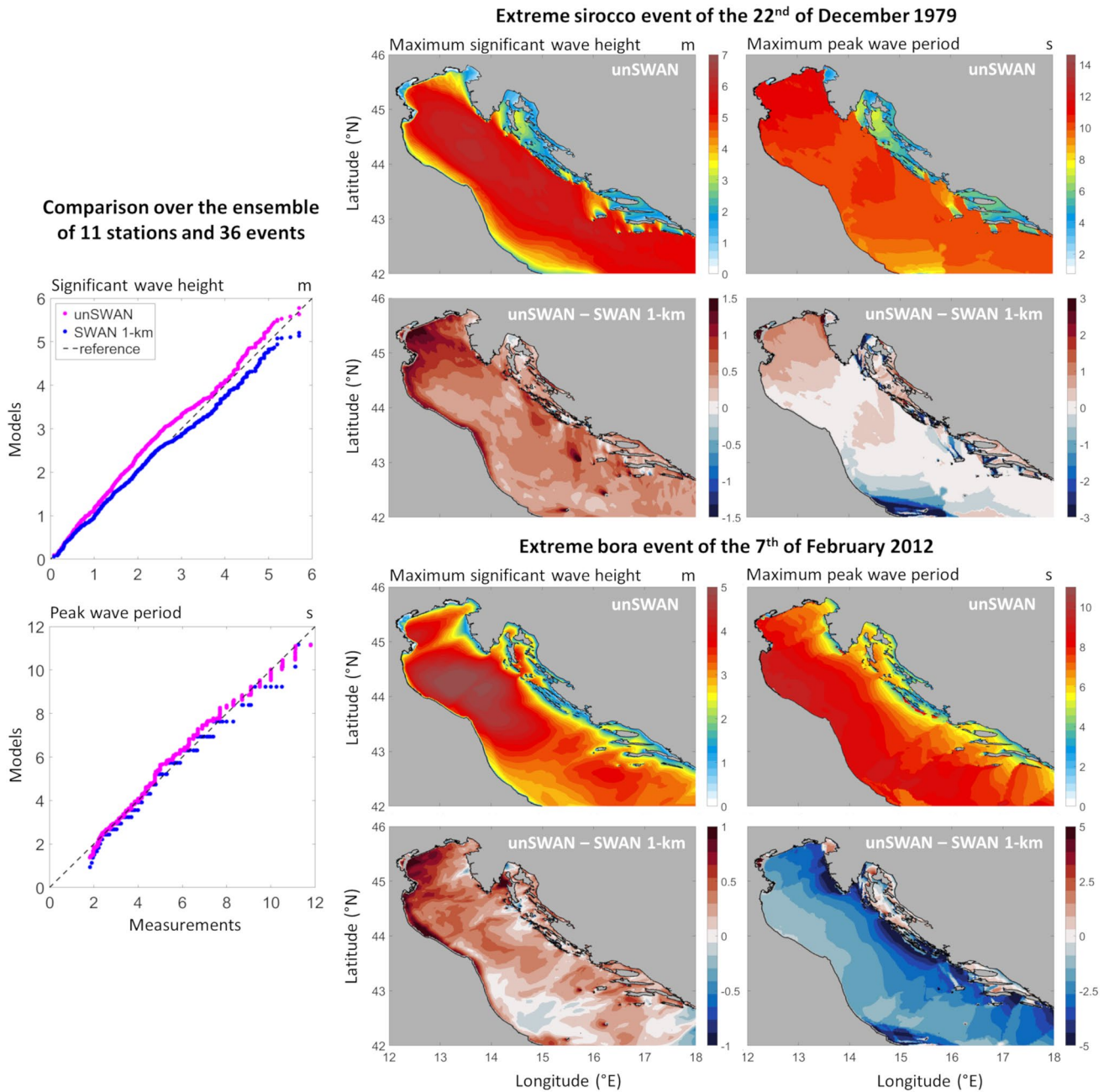


Fig. 17 Analysis of the sensitivity of the wave results to model resolution: with quantile–quantile distributions of the AdriSC SWAN 1-km and unSWAN results vs. measurements for the ensemble of 9 stations and 36 extreme events (left panels) and with spatial distributions of unSWAN results and differences between unSWAN and SWAN 1-km results for the maximum significant wave height and the maximum peak wave period during one extreme sirocco event (22 December 1979) and one extreme bora event (7 February 2012)

istributions of unSWAN results and differences between unSWAN and SWAN 1-km results for the maximum significant wave height and the maximum peak wave period during one extreme sirocco event (22 December 1979) and one extreme bora event (7 February 2012)

(in Croatian), local newspapers, photographs and videos, was thus undertaken to generate the ensemble of 22 historical bora storms used in this study.

Table 4 References used to select the date of the 22 representative extreme bora events of the ensemble

Event	Reference: research articles, meteorological bulletins, news reports and videos
24/11/1991	Brzović and Benković (1994)
28/12/1992	Ivančan-Picek and Tutiš (1996)
01/02/1994	Bilten iz područja meteorologije, hidrologije, primijenjene meteorologije i zaštite čovjekova okoliša, https://meteo.hr/proizvodi.php?section=publikacije&param=publikacije_publicacij_e_dhmz&el=bilteni
16/02/1997	
09/03/1998	Brzović (1999)
28/03/1995	
30/03/1995	
21/12/1998	Bajić and Glasnović (1999)
07/11/1999	Klaić et al. (2003)
14/11/2004	Belušić and Klaić (2006)
15/12/2007	https://www.istramet.hr/vijesti/15122006-snijeg-se-zadržao-i-tokom-dana/
10/03/2010	https://www.tportal.hr/vijesti/clanak/orkanska-bura-otkinula-komad-krova-skole-20100310
02/03/2011	https://www.tportal.hr/vijesti/clanak/orkanska-bura-nosi-sve-pred-sobom-20110302
07/02/2012	Ličer et al. (2016)
11/02/2012	
11/11/2013	https://rijeka.meteoadriatic.net/vremeplov-orkanska-bura-u-rijeci-i-na-kvarneru-11-11-2013/
31/12/2014	https://www.youtube.com/watch?v=0kNlrL_diFY
01/01/2015	
05/03/2015	https://www.crometeo.hr/orkanska-bura-na-jadraniu-foto-video/
17/01/2017	https://www.tportal.hr/vijesti/clanak/snazna-bura-u-istri-stvara-velike-teskoce-20170117
13/11/2017	https://www.tportal.hr/vijesti/clanak/bura-otrgnula-novi-brod-i-zabila-ga-u-mol-u-puli-foto-20171113
24/09/2018	https://www.tportal.hr/vijesti/clanak/orkanska-bura-srucila-se-na-split-kontejneri-setaju-ulicama-problemi-u-pomorskom-prometu-ali-i-na-nebu-foto-20180924

References

- Adloff F, Jordà G, Somot S, Sevault F, Arsouze T, Meyssignac B, Li L, Planton S (2018) Improving sea-level simulation in Mediterranean regional climate models. *Clim Dyn* 51:1167–1178. <https://doi.org/10.1007/s00382-017-3842-3>
- Androulidakis YS, Kombiadou KD, Makris CV, Baltikas VN, Krestenitis YN (2015) Storm surges in the Mediterranean Sea: variability and trends under future climatic conditions. *Dyn Atmos Oceans* 71:56–82. <https://doi.org/10.1016/j.dynatmoce.2015.06.001>
- Argueso D, Evans JP, Fita L, Bormann KJ (2014) Temperature response to future urbanization and climate change. *Clim Dyn* 42:2183–2199. <https://doi.org/10.1007/s00382-013-1789-6>
- Bajić A, Glasnović D (1999) Impact of Adriatic Bora on traffic. In: Proceedings from the 4th European conference on applied meteorology, Norrköping, SMHI
- Bajo M, Medugorac I, Umgiesser G, Orlić M (2019) Storm surge and seiche modelling in the Adriatic Sea and the impact of data assimilation. *Q J R Meteorol Soc* 145:2070–2084. <https://doi.org/10.1002/qj.3544>
- Balsamo G, Albergel C, Beljaars A, Boussetta S, Brun E, Cloke H, Dee D, Dutra E, Muñoz-Sabater J, Pappenberger F, de Rosnay P, Stockdale T, Vitart F (2015) ERA-Interim/Land: a global land surface reanalysis data set. *Hydrol Earth Syst Sci* 19:389–407. <https://doi.org/10.5194/hess-19-389-2015>
- Ban N, Schmidli J, Schär C (2014) Evaluation of the convection-resolving regional climate modeling approach in decade-long simulations. *J Geophys Res Atmos* 119:7889–7907. <https://doi.org/10.1002/2014JD021478>
- Ban N, Schmidli J, Schär C (2015) Heavy precipitation in a changing climate: does short-term summer precipitation increase faster? *Geophys Res Lett* 42:1165–1172. <https://doi.org/10.1002/2014GL062588>
- Bellafiore D, Bucchignani E, Gualdi S, Carniel S, Djurdjević V, Umgiesser G (2012) Assessment of meteorological climate models as inputs for coastal studies. *Ocean Dyn* 62:555–568. <https://doi.org/10.1007/s10236-011-0508-2>
- Belušić D, Klaić ZB (2006) Mesoscale dynamics, structure and predictability of a severe Adriatic bora case. *Meteorol Z* 15:157–168
- Belušić A, Prtenjak MT, Güttler I, Ban N, Leutwyler D, Schär C (2017) Near-surface wind variability over the broader Adriatic region: insights from an ensemble of regional climate models. *Clim Dyn* 50:4455–4480. <https://doi.org/10.1007/s00382-017-3885-5>
- Belušić Vozila A, Güttler I, Ahrens B, Obermann-Hellhund A, Telišman Prtenjak M (2019) Wind over the Adriatic region in CORDEX climate change scenarios. *J Geophys Res Atmos* 124:110–130. <https://doi.org/10.1029/2018JD028552>
- Bencivenga M, Nardone G, Ruggiero F, Calore D (2012) The Italian Data Buoy Network (RON). *Adv Fluid Mech IX*, WIT Trans Eng Sci 74:321–332
- Benetazzo A, Fedele F, Carniel S, Ricchi A, Bucchignani E, Sclavo M (2012) Wave climate of the Adriatic Sea: a future scenario simulation. *Nat Hazards Earth Syst Sci* 12:2065–2076. <https://doi.org/10.5194/nhess-12-2065-2012>
- Bernstein L, Bosch P, Canziani O, Chen Z, Christ R, Riahi K (2008) IPCC, 2007: climate change 2007: synthesis report. IPCC, Geneva. ISBN 2-9169-122-4
- Bertotti L, Bidlot J-R, Buizza R, Cavaleri L, Janousek M (2011) Deterministic and ensemble-based prediction of Adriatic Sea sirocco storms leading to ‘acqua alta’ in Venice. *Q J R Meteorol Soc* 137:1446–1466. <https://doi.org/10.1002/qj.861>
- Beuquier J, Sevault F, Herrmann M, Kontoyiannis H, Ludwig W, Rixen M, Stanev E, Béranger K, Somot S (2010) Modeling the

- Mediterranean Sea interannual variability during 1961–2000: focus on the Eastern Mediterranean Transient. *J Geophys Res Atmos* 115:C08017. <https://doi.org/10.1029/2009JC005950>
- Biolchi S, Furlani S, Devoto S, Scicchitano G, Korbar T, Vilibić I, Šepić J (2019a) The origin and dynamics of coastal boulders in a semi-enclosed shallow basin: a northern Adriatic case study. *Mar Geol* 411:62–77. <https://doi.org/10.1016/j.margeo.2019.01.008>
- Biolchi S, Denamiel C, Devoto S, Korbar T, Macovaz V, Scicchitano G, Vilibić I, Furlani S (2019b) Impact of the October 2018 Storm Vaia on coastal boulders in the northern Adriatic Sea. *Water* 11:2229. <https://doi.org/10.3390/w11112229>
- Bonaldo D, Bucchignani E, Ricchi A, Carniel S (2017) Wind storminess in the Adriatic Sea in a climate change scenario. *Acta Adriat* 58(2):195–208
- Brogli R, Sørland SL, Krøner N, Schär C (2019a) Causes of future Mediterranean precipitation decline depend on the season. *Environ Res Lett* 14:114017. <https://doi.org/10.1088/1748-9326/ab4438>
- Brogli R, Krøner N, Sørland SL, Lüthi D, Schär C (2019b) The role of Hadley circulation and lapse-rate changes for the future European summer climate. *J Clim* 32:385–404. <https://doi.org/10.1175/JCLI-D-18-0431.1>
- Brzović N (1999) Factors affecting the Adriatic cyclone and associated windstorms. *Contrib Atmos Phys* 72:51–65
- Brzović N, Benković M (1994) Severe Adriatic bora storms 1987–1993. *Croat Meteorol J* 29:65–74. <https://hrcak.srce.hr/69265>
- Brzović N, Strelec Mahović N (1999) Cyclonic activity and severe Jugo in the Adriatic. *Phys Chem Earth B* 24(6):653–657. [https://doi.org/10.1016/S1464-1909\(99\)00061-1](https://doi.org/10.1016/S1464-1909(99)00061-1)
- Cavaleri L (2000) The oceanographic tower Acqua Alta activity and prediction of sea states at Venice. *Coast Eng* 39(1):29–70. [https://doi.org/10.1016/S0378-3839\(99\)00053-8](https://doi.org/10.1016/S0378-3839(99)00053-8)
- Cavaleri L, Bertotti L, Buizza R, Buzzi A, Masato V, Umgiesser G, Zampieri M (2010) Predictability of extreme meteo-oceanographic events in the Adriatic Sea. *Q J R Meteorol Soc* 136:400–413. <https://doi.org/10.1002/qj.567>
- Cavaleri L, Abdalla S, Benetazzo A, Bertotti L, Bidlot J-R, Breivik Ø, Carniel S, Jensen RE, Portilla-Yandun J, Rogers WE, Roland A, Sanchez-Arcilla A, Smith JM, Staneva J, Toledo Y, van Vledder GPh, van der Westhuysen AJ (2018) Wave modelling in coastal and inner seas. *Prog Oceanogr* 167:164–233. <https://doi.org/10.1016/j.pocean.2018.03.010>
- Cavaleri L, Bajo M, Barbariol F, Bastianini M, Benetazzo A, Bertotti L, Chiggiato J, D'Avolio S, Ferrarin C, Magnusson L, Papa A, Pezzutto P, Pomaro A, Umgiesser G (2019) The October 29, 2018 storm in Northern Italy—an exceptional event and its modeling. *Prog Oceanogr* 178:102178. <https://doi.org/10.1016/j.pocean.2019.102178>
- Cushman-Roisin B, Gačić M, Poulain P-M, Artegiani A (2001) Physical oceanography of the Adriatic Sea: past, present and future. Springer, New York
- Dee DP, Uppala SM, Simmons AJ, Berrisford P, Poli P, Kobayashi S, Andrae U, Balmaseda MA, Balsamo G, Bauer P, Bechtold P, Beljaars ACM, van de Berg L, Bidlot J, Bormann N, Delsol C, Dragani R, Fuentes M, Geer AJ, Haimberger L, Healy SB, Hersbach H, Hólm EV, Isaksen L, Kållberg P, Köhler M, Matricardi M, McNally AP, Monge-Sanz BM, Morcrette JJ, Park BK, Peubey C, de Rosnay P, Tavolato C, Thépaut JN, Vitart F (2011) The ERA-Interim reanalysis: configuration and performance of the data assimilation system. *Q J R Meteorol Soc* 137:553–597. <https://doi.org/10.1002/qj.828>
- Denamiel C, Šepić J, Ivanković D, Vilibić I (2019) The Adriatic Sea and Coast modelling suite: evaluation of the meteotsunami forecast component. *Ocean Model* 135:71–93. <https://doi.org/10.1016/j.ocemod.2019.02.003>
- Dietrich JC, Tanaka S, Westerink JJ, Dawson CN, Luettich RA Jr, Zijlema M, Holthuijsen LH, Smith JM, Westerink JG, Westerink HJ (2012) Performance of the Unstructured-Mesh, SWAN+ADCIRC Model in computing hurricane waves and surge. *J Sci Comput* 52:468–497. <https://doi.org/10.1007/s10915-011-9555-6>
- Fosser G, Khodayar S, Berg P (2016) Climate change in the next 30 years: what can a convection-permitting model tell us that we did not already know? *Clim Dyn* 48:1987–2003. <https://doi.org/10.1007/s00382-016-3186-4>
- Giorgi F, Gutowski WJ (2015) Regional dynamical downscaling and the CORDEX initiative. *Ann Rev Environ Resour* 40(1):467–490. <https://doi.org/10.1146/annurev-environ-102014-021217>
- Giorgi F, Jones C, Asrar G (2009) Addressing climate information needs at the regional level: the CORDEX framework. *WMO Bull* 58(3):175–183
- Gohm A, Mayr GJ, Fix A, Giez A (2008) On the onset of bora and the formation of rotors and jumps near a mountain gap. *Q J R Meteorol Soc* 134:21–46. <https://doi.org/10.1002/qj.206>
- Grisogono B, Belušić D (2009) A review of recent advances in understanding the meso- and microscale properties of the severe Bora wind. *Tellus A* 61:1–16. <https://doi.org/10.1111/j.1600-0870.2008.00369.x>
- Gualdi S, Somot S, Li L, Artale V, Adani M, Bellucci A, Braun A, Calmanti S, Carillo A, Dell'Aquila A, Déqué M, Dubois C, Elizalde A, Harzallah A, Jacob D, L'Hévéder B, May W, Oddo P, Ruti P, Sanna A, Sannino G, Scoccimarro E, Sevault F, Navarra A (2013) The CIRCE simulations: regional climate change projections with realistic representation of the Mediterranean Sea. *Bull Am Meteorol Soc* 94:65–81. <https://doi.org/10.1175/BAMS-D-11-00136.1>
- Han G, Ma Z, Long Z, Perrie W, Chassé J (2019) Climate change on Newfoundland and Labrador shelves: results from a regional downscaled ocean and sea-ice model under an A1B forcing scenario 2011–2069. *Atmos Ocean* 57(1):3–17. <https://doi.org/10.1080/07055900.2017.1417110>
- Hintze HL, Nelson RD (1998) Violin plots: a box plot-density trace synergism. *Am Stat* 52(2):181–184. <https://doi.org/10.1080/00031305.1998.10480559>
- Hourdin F, Musat I, Bony S, Braconnot P, Codron F, Dufresne JL, Fairhead L, Filiberti MA, Friedlingstein P, Grandpeix JY, Krinner G, LeVan P, Li ZX, Lott F (2006) The LMDZ4 general circulation model: climate performance and sensitivity to parametrized physics with emphasis on tropical convection. *Clim Dyn* 27:787–813. <https://doi.org/10.1007/s00382-006-0158-0>
- Ivančan-Picek B, Tutiš V (1996) A case study of a severe Adriatic bora on 28 December 1992. *Tellus A* 48:357–367. <https://doi.org/10.3402/tellusa.v48i3.12065>
- Janeković I, Mihanović H, Vilibić I, Tudor M (2014) Extreme cooling and dense water formation estimates in open and coastal regions of the Adriatic Sea during the winter of 2012. *J Geophys Res Oceans* 119:3200–3218. <https://doi.org/10.1002/2014JC009865>
- Jenkins C, Trincardi F, Hatchett L, Nedoroda A, Goff J, Signell R, McKinney K (2005) <http://instaar.colorado.edu/~jenkinsc/dbseabed/coverage/adriaticsea/adriatico.htm>
- Jiang Q, Doyle JD (2005) Wave breaking induced surface wakes and jets observed during a bora event. *Geophys Res Lett* 32:L17807. <https://doi.org/10.1029/2005GL022398>
- Johns B, Rao AD, Dubinsky Z, Sinha PC (1985) Numerical modelling of tide-surge interaction in the Bay of Bengal. *Philos Trans R Soc Lond Ser A Math Phys Sci* 313(1526):507–535. <https://doi.org/10.1098/rsta.1985.0002>
- Jordà G, Gomis D (2013) On the interpretation of the steric and mass components of sea-level variability: the case of the Mediterranean basin. *J Geophys Res Oceans* 118:953–963. <https://doi.org/10.1002/jgrc.20060>

- Josipović L, Obermann-Hellhund A, Brisson E, Ahrens B (2018) Bora in regional climate models: impact of model resolution on simulations of gap wind and wave breaking. *Croat Meteorol J* 53:31–42. <https://hrcak.srce.hr/231266>
- Jurčec V, Ivančan-Picek B, Tutiš V, Vukičević V (1996) Severe Adriatic jugo wind. *Meteorol Z* 5:67–75
- Kendon EJ, Fowler HJ, Roberts MJ, Chan SC, Senior CA (2014) Heavier summer downpours with climate change revealed by weather forecast resolution model. *Nat Clim Change* 4:570–576. <https://doi.org/10.1038/nclimate2258>
- Kendon EJ, Ban N, Roberts NM, Fowler HJ, Roberts MJ, Chan SC, Evans JP, Fosser G, Wilkinson JM (2017) Do convection-permitting regional climate models improve projections of future precipitation change? *Bull Am Meteorol Soc* 98:79–93. <https://doi.org/10.1175/BAMS-D-15-0004.1>
- Klaić ZB, Belušić D, Grubišić V, Gabela L, Čoso L (2003) Mesoscale airflow structure over the northern Croatian coast during MAP IOP15—a major bora event. *Geofizika* 20:23–60
- Klaić ZB, Prodanov AD, Belušić D (2009) Wind measurements in Senj: underestimation of true bora flows. *Geofizika* 26:245–252
- Komen GJ, Hasselmann S, Hasselmann K (1984) On the existence of a fully developed wind-sea spectrum. *J Phys Oceanogr* 14:1271–1285. [https://doi.org/10.1175/1520-0485\(1984\)014%3c1271:OTEOAF%3e2.0.CO;2](https://doi.org/10.1175/1520-0485(1984)014%3c1271:OTEOAF%3e2.0.CO;2)
- Kröner N, Kotlarski S, Fischer E, Lüthi D, Zubler E, Schär C (2017) Separating climate change signals into thermodynamic, lapse-rate and circulation effects: theory and application to the European summer climate. *Clim Dyn* 48:3425–3440. <https://doi.org/10.1007/s00382-016-3276-3>
- Kuzmić M, Janeković I, Ivančan-Picek B, Trošić T, Tomažić I (2005) Severe northeastern Adriatic bura events and circulation in greater Kvarner region. *Croat Meteorol J* 40:320–323
- Leder N, Smirčić A, Vilibić I (1998) Extreme values of surface wave heights in the Northern Adriatic. *Geofizika* 15:1–13
- Li Y, Li Z, Zhang Z, Chen L, Kurkute S, Scaff L, Pan X (2019) High-resolution regional climate modeling and projection over western Canada using a weather research forecasting model with a pseudo-global warming approach. *Hydrol Earth Syst Sci* 23(11):4635–4659. <https://doi.org/10.5194/hess-23-4635-2019>
- Ličer M, Smerkol P, Fettich A, Ravdas M, Papapostolou A, Mantzi-afou A, Strajnar B, Cedilnik J, Jeromel M, Jerman J, Petan S, Malačič V, Sofianos S (2016) Modeling the ocean and atmosphere during an extreme bora event in northern Adriatic using one-way and two-way atmosphere–ocean coupling. *Ocean Sci* 12:71–86. <https://doi.org/10.5194/os-12-71-2016>
- Lionello P, Cavaleri L, Nissen KM, Pino C, Raicich F, Ulbrich U (2012a) Severe marine storms in the Northern Adriatic: characteristics and trends. *Phys Chem Earth* 40(41):93–105. <https://doi.org/10.1016/j.pce.2010.10.002>
- Lionello P, Galati MB, Elvini E (2012b) Extreme storm surge and wind wave climate scenario simulations at the Venetian littoral. *Phys Chem Earth* 40(41):86–92. <https://doi.org/10.1016/j.pce.2010.04.001>
- Ludwig W, Dumont E, Meybeck M, Heussner S (2009) River discharges of water and nutrients to the Mediterranean and Black Sea: major drivers for ecosystem changes during past and future decades? *Prog Oceanogr* 80(3–4):199–217. <https://doi.org/10.1016/j.pocean.2009.02.001>
- Macias D, Stips A, Garcia-Gorrioz E, Dosio A (2018) Hydrological and biogeochemical response of the Mediterranean Sea to freshwater flow changes for the end of the 21st century. *PLoS One* 13(2):e0192174. <https://doi.org/10.1371/journal.pone.0192174>
- Madsen OS, Poon Y-K, Graber HC (1988) Spectral wave attenuation by bottom friction: theory. In: *Proceedings of the 21st international conference on coastal engineering*, ASCE, pp 492–504
- Međugorac I, Pasarić M, Orlić M (2015) Severe flooding along the eastern Adriatic coast: the case of 1 December 2008. *Ocean Dyn* 65:817–830. <https://doi.org/10.1007/s10236-015-0835-9>
- Mel R, Sterl A, Lionello P (2013) High resolution climate projection of storm surge at the Venetian coast. *Nat Hazards Earth Syst Sci* 13:1135–1142. <https://doi.org/10.5194/nhess-13-1135-2013>
- Pan L-L, Chen S-H, Cayan D, Lin M-Y, Hart Q, Zhang M-H, Liu Y, Wang J (2011) Influences of climate change on California and Nevada regions revealed by a high-resolution dynamical downscaling study. *Clim Dyn* 37:2005–2020. <https://doi.org/10.1007/s00382-010-0961-5>
- Parker BB (1991) The Relative Importance of the various nonlinear mechanisms in a wide range of tidal interaction (review). *Tidal hydrodynamics*. Wiley, New York, pp 237–268
- Pasarić M, Orlić M (2004) Meteorological forcing of the Adriatic: present vs. projected climate conditions. *Geofizika* 21:69–86
- Pasarić Z, Belušić D, Klaić ZB (2007) Orographic influences on the Adriatic sirocco wind. *Ann Geophys* 25:1263–1267
- Penzar B, Penzar I, Orlić M (2001) Vrijeme i klima hrvatskog Jadrana. *Nakladna kuća. 'Dr. Feletar', Zagreb*
- Pinardi N, Allen I, Demirov E, De Mey P, Korres G, Lascaratos A, Le Traon P-Y, Maillard C, Manzella G, Tziavos C (2003) The Mediterranean ocean Forecasting System: first phase of implementation (1998–2001). *Ann Geophys* 21:3–20. <https://doi.org/10.5194/angeo-21-3-2003>
- Poje D (1992) Wind persistence in Croatia. *Int J Climatol* 12:569–586
- Pomaro A, Cavaleri L, Lionello P (2017) Climatology and trends of the Adriatic Sea wind waves: analysis of a 37-year long instrumental data set. *Int J Climatol* 37:4237–4250. <https://doi.org/10.1002/joc.5066>
- Pomaro A, Cavaleri L, Papa A, Lionello P (2018) 39 years of directional wave recorded data and relative problems, climatological implications and use. *Sci Data* 5:180139. <https://doi.org/10.1038/sdata.2018.139>
- Prein AF, Langhans W, Fosser G, Ferrone A, Ban N, Goergen K, Keller M, Tölle M, Gutjahr O, Feser F, Brisson E, Kollet S, Schmidli J, van Lipzig NPM, Leung R (2015) A review on regional convection-permitting climate modeling: demonstrations, prospects and challenges. *Rev Geophys* 53:323–361. <https://doi.org/10.1002/2014RG000475>
- Prtenjak MT, Belušić D (2009) Formation of reversed lee flow over the north-eastern Adriatic during bora. *Geofizika* 26:145–155
- Prtenjak MT, Viher M, Jurković J (2010) Sea-land breeze development during a summer bora event along the north-eastern Adriatic coast. *Q J R Meteorol Soc* 136:1554–1571. <https://doi.org/10.1002/qj.649>
- Pullen J, Doyle JD, Signell RP (2006) Two-way air–sea coupling: a study of the Adriatic. *Mon Weather Rev* 134:1465–1483. <https://doi.org/10.1175/MWR3137.1>
- Raicich F (2015) Long-term variability of storm surge frequency in the Venice Lagoon: an update thanks to 18th century sea-level observations. *Nat Hazards Earth Syst Sci* 15:527–535. <https://doi.org/10.5194/nhess-15-527-2015>
- Rasmussen R, Liu C, Ikeda K, Gochis D, Yates D, Chen F, Tewari M, Barlage M, Dudhia J, Yu W, Miller K, Arsenault K, Grubišić V, Thompson G, Gutmann E (2011) High-resolution coupled climate runoff simulations of seasonal snowfall over Colorado: a process study of current and warmer climate. *J Clim* 24:3015–3048. <https://doi.org/10.1175/2010JCLI3985.1>
- Rasmussen R, Ikeda K, Liu C, Gochis D, Clark M, Dai A, Gutmann E, Dudhia J, Chen F, Barlage M, Yates D, Zhang G (2014) Climate change impacts on the water balance of the Colorado headwaters: High-resolution regional climate model simulations. *J Hydrometeorol* 15:1091–1116. <https://doi.org/10.1175/JHM-D-13-0118.1>
- Ravdas M, Zacharioudaki A, Korres G (2018) Implementation and validation of a new operational wave forecasting system of

- the Mediterranean Monitoring and Forecasting Centre in the framework of the Copernicus Marine Environment Monitoring Service. *Nat Hazards Earth Syst Sci* 18:2675–2695. <https://doi.org/10.5194/nhess-18-2675-2018>
- Ricchi A, Miglietta MM, Falco PP, Benetazzo A, Bonaldo D, Bergamasco A, Sclavo M, Carniel S (2016) On the use of a coupled ocean–atmosphere–wave model during an extreme cold air outbreak over the Adriatic Sea. *Atmos Res* 172–173:48–65. <https://doi.org/10.1016/j.atmosres.2015.12.023>
- Rizzi J, Torresan S, Zabeo A, Critto A, Tosoni A, Tomasin A, Marcomini A (2017) Assessing storm surge risk under future sea-level rise scenarios: a case study in the North Adriatic coast. *J Coast Conserv* 21:453–471. <https://doi.org/10.1007/s1185-0217-0517-5>
- Robinson AR, Tomasin A, Artegiani A (1973) Flooding of Venice: phenomenology and prediction of the Adriatic Sea storm surge. *Q J R Meteorol Soc* 99:688–692. <https://doi.org/10.1002/qj.49709942210>
- Ruti PM, Somot S, Giorgi F, Dubois C, Flaounas E, Obermann A, Dell’Aquila A, Pisacane G, Harzallah A et al (2016) MedCORDEX initiative for Mediterranean climate studies. *Bull Am Meteorol Soc* 97:1187–1208. <https://doi.org/10.1175/BAMS-D-14-00176.1>
- Schär C, Frei C, Luthi D, Davies HC (1996) Surrogate climate-change scenarios for regional climate models. *Geophys Res Lett* 23:669–672. <https://doi.org/10.1029/96GL00265>
- Speer PE, Aubrey DG (1985) A study of non-linear tidal propagation in shallow inlet/estuarine systems. Part II: theory. *Estuar Coast Shelf Sci* 21(2):207–224. [https://doi.org/10.1016/0272-7714\(85\)90097-6](https://doi.org/10.1016/0272-7714(85)90097-6)
- Tinker J, Lowe J, Pardaens A, Holt J, Rosa Barciela (2016) Uncertainty in climate projections for the 21st century northwest European shelf seas. *Prog Oceanogr* 148:56–73. <https://doi.org/10.1016/j.pocean.2016.09.003>
- Tolle MH, Gutjahr O, Busch G, Thiele JC (2014) Increasing bioenergy production on arable land: does the regional and local climate respond? Germany as a case study. *J Geophys Res Atmos* 119:2711–2724. <https://doi.org/10.1002/2013JD020877>
- Torresan S, Gallina V, Gualdi S, Bellafiore D, Umgiesser G, Carniel S, Sclavo M, Benetazzo A, Giubilato E, Critto A (2019) Assessment of climate change impacts in the North Adriatic coastal area. Part I: a multi-model chain for the definition of climate change hazard scenarios. *Water* 11:1157. <https://doi.org/10.3390/w11061157>
- Trigo IF, Davies TD (2002) Meteorological conditions associated with sea surges in Venice: a 40 year climatology. *Int J Climatol* 22:787–803. <https://doi.org/10.1002/joc.719>
- Trošić T (2015) The onset of a severe summer bora episode near Oštarijska Vrata Pass in the Northern Adriatic. *Meteorol Atmos Phys* 127:649–658. <https://doi.org/10.1007/s00703-015-0393-1>
- Tsimplis M, Marcos M, Somot S, Barnier B (2008) Sea-level forcing in the Mediterranean Sea between 1960 and 2000. *Glob Planet Change* 63(4):325–332. <https://doi.org/10.1016/j.gloplacha.2008.07.004>
- Vilibić I, Šepić J, Proust N (2013) Weakening thermohaline circulation in the Adriatic Sea. *Clim Res* 55(3):217–225. <https://doi.org/10.3354/cr01128>
- Vilibić I, Šepić J, Pasarić M, Orlić M (2017) The Adriatic Sea: a long-standing laboratory for sea-level studies. *Pure Appl Geophys* 174:3765–3811. <https://doi.org/10.1007/s00024-017-1625-8>
- Warner JC, Armstrong B, He R, Zambon JB (2010) Development of a Coupled Ocean-Atmosphere-Wave-Sediment Transport (COAWST) modeling system. *Ocean Model* 35:230–244. <https://doi.org/10.1016/j.ocemod.2010.07.010>
- Yang W, Yin B, Feng X, Yang D, Gao G, Chen H (2019) The effect of nonlinear factors on tide-surge interaction: a case study of Typhoon Rammasun in Tieshan Bay, China. *Estuar Coast Shelf Sci* 219:420–428. <https://doi.org/10.1016/j.ecss.2019.01.024>
- Zhang H, Cheng W, Qiu X, Feng X, Gong W (2017) Tide-surge interaction along the east coast of the Leizhou Peninsula, south China sea. *Cont Shelf Res* 142:32–49. <https://doi.org/10.1016/j.csr.2017.05.015>
- Zou L, Zhou T (2016) A regional ocean–atmosphere coupled model developed for CORDEX East Asia: assessment of Asian summer monsoon simulation. *Clim Dyn* 47:3627–3640. <https://doi.org/10.1007/s00382-016-3032-8>

Publisher’s Note Springer Nature remains neutral with regard to jurisdictional claims in published maps and institutional affiliations.